Nonequilibrium spin dynamics in systems of ultracold atoms

Eugene Demler Harvard University

Collaborators:
Ehud Altman, Robert Cherng, Vladimir Gritsev, Mikhail Lukin, Anatoli Polkovnikov, Ana Maria Rey

Experimental collaborators:
Immanuel Bloch's group and Dan Stamper-Kurn's group

Funded by NSF, DARPA, MURI, AFOSR, Harvard-MIT CUA

Outline

Dipolar interactions in spinor condensates

arXiv:0806.1991

Larmor precession and dipolar interactions. Roton instabilities.

Following experiments of D. Stamper-Kurn

Many-body decoherence and Ramsey interferometry

Phys. Rev. Lett. 100:140401 (2008)

Luttinger liquids and non-equilibrium dynamics.

Collaboration with I. Bloch's group.

Superexchange interaction in double well systems

Science 319:295 (2008)

Towards quantum magnetism of ultracold atoms.

Collaboration with I. Bloch's group.

Dipolar interactions in spinor condensates.

Roton softening and possible supersolid phase

R. Cherng and E. Demler, arXiv:0806.1991

Theory of the Superfluidity of Helium II

L. Landau

From these properties of the energy spectrum the heat capacity of helium II must consist of two parts: the "phonon part," i.e., the normal Debye heat capacity proportional to T^4, and the "roton part," depending on the temperature exponentially $(\sim e^{-\Delta/kT})$.

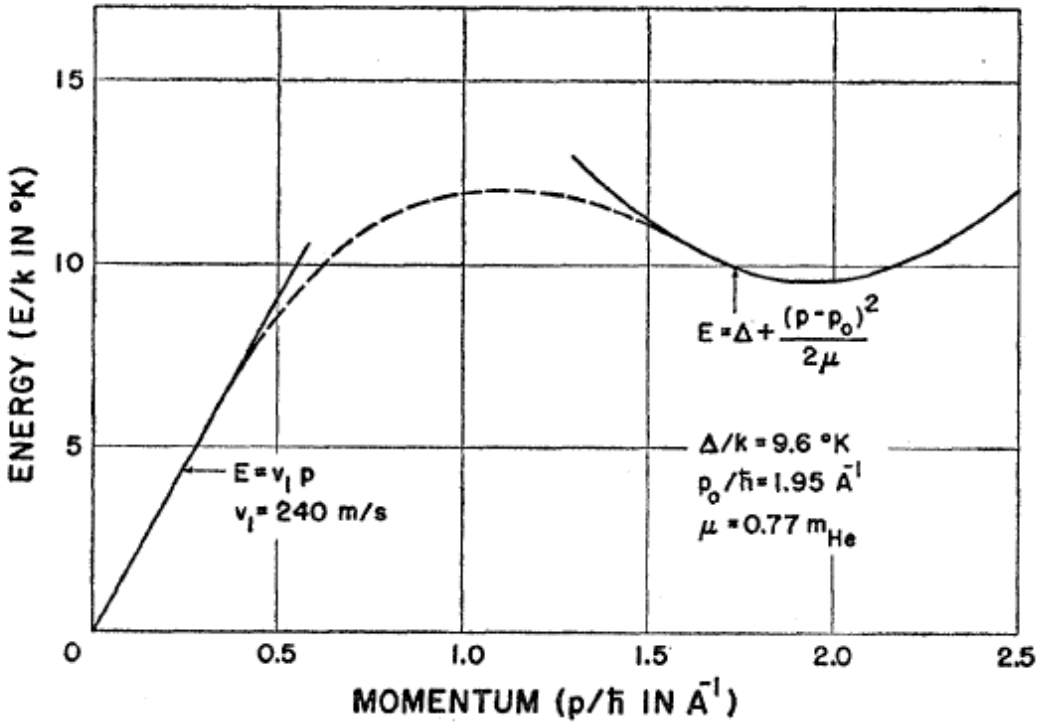

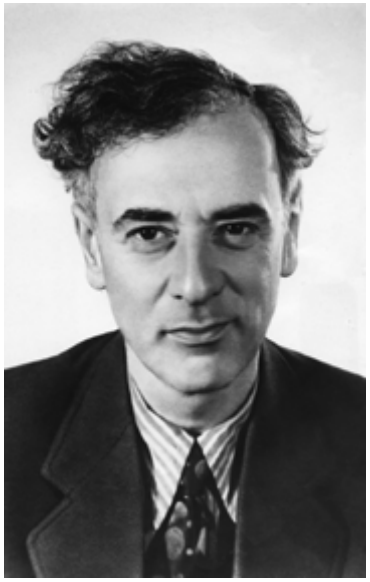

Excitations in Liquid Helium: Neutron Scattering Measurements*

J. L. YARNELL, G. P. ARNOLD, P. J. BENDT, AND E. C. KERR

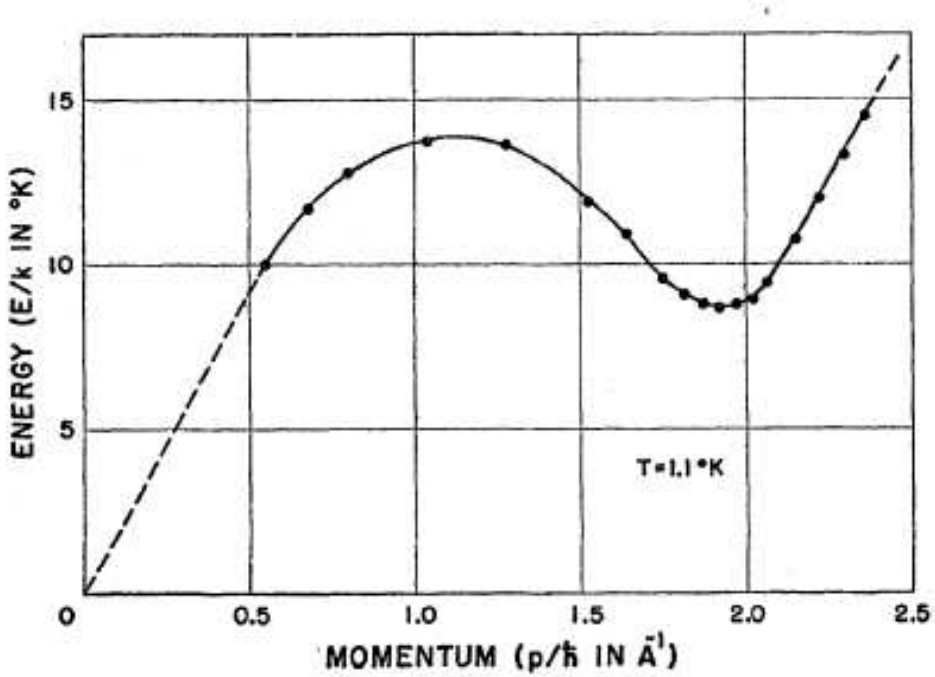

FIG. 8. The energy spectrum of the excitations in liquid helium at 1.1°K. The dashed line joining the origin and the first measured point has a slope corresponding to a first sound velocity of 239 ± 5 meters/sec. The maximum occurs at $p/\hbar=1.11\pm0.04$ A^{-1}, $E/k=13.92\pm0.10$°K. The region of the minimum is shown in greater detail in Fig. 9.

Possible supersolid phase in ^{4}He

Phase diagram of 4He

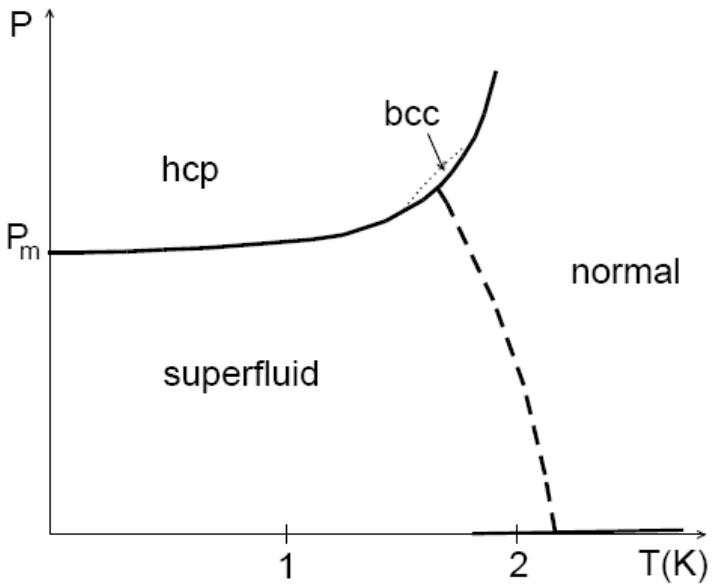

A.F. Andreev and I.M. Lifshits (1969):
Melting of vacancies in a crystal due to strong quantum fluctuations.

Also
G. Chester (1970); A.J. Leggett (1970)

Kirzhnits, Nepomnyashchii (1970); Schneider, Enz (1971).

Formation of the supersolid phase due to softening of roton excitations

Probable observation of a supersolid helium phase

E. Kim & M. H. W. Chan

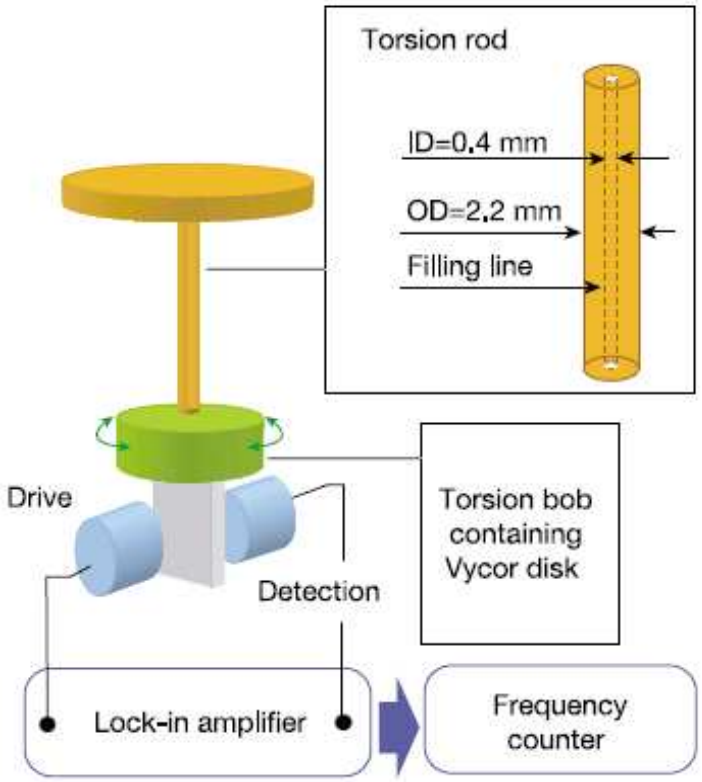

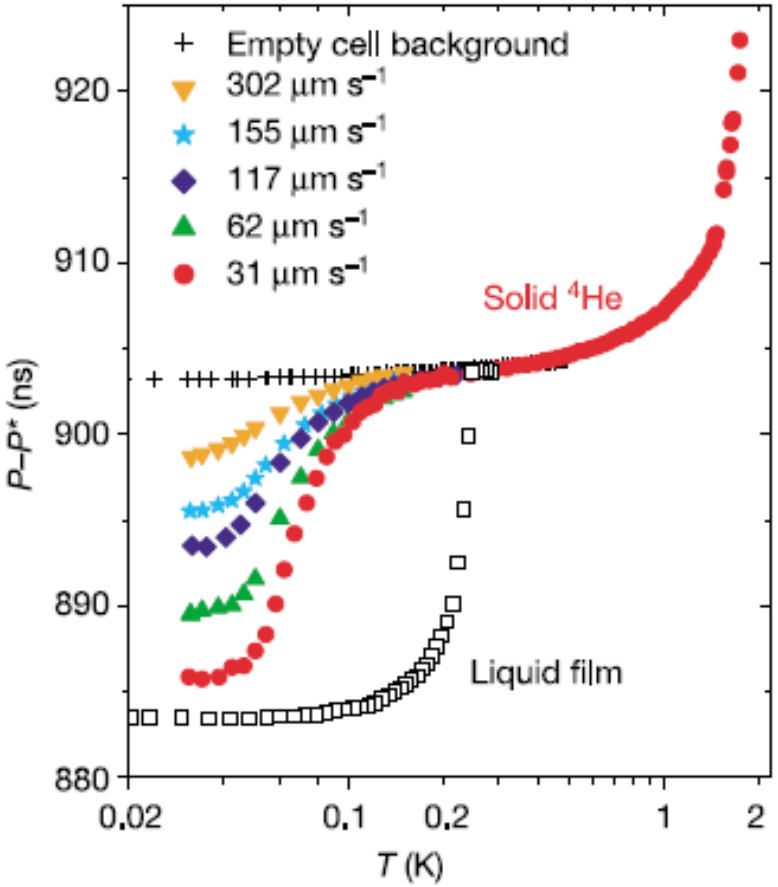

Resonant period as a function of T

Interlayer coherence in bilayer quantum Hall systems at ν=1

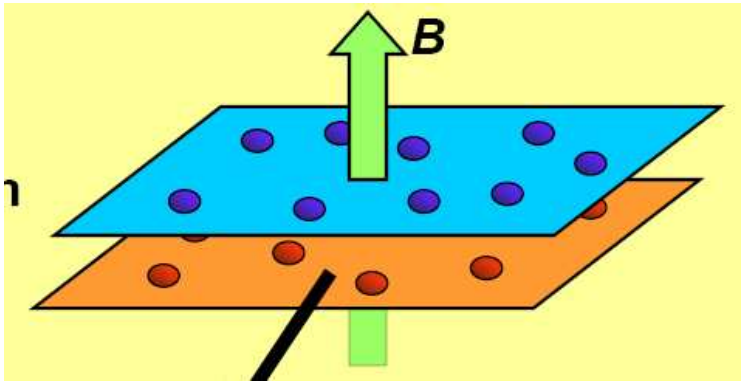

Hartree-Fock predicts roton softening and transition into a state with both interlayer coherence and stripe order. Transport experiments suggest first order transition into a compressible state.

Eisenstein, Boebinger et al. (1994)

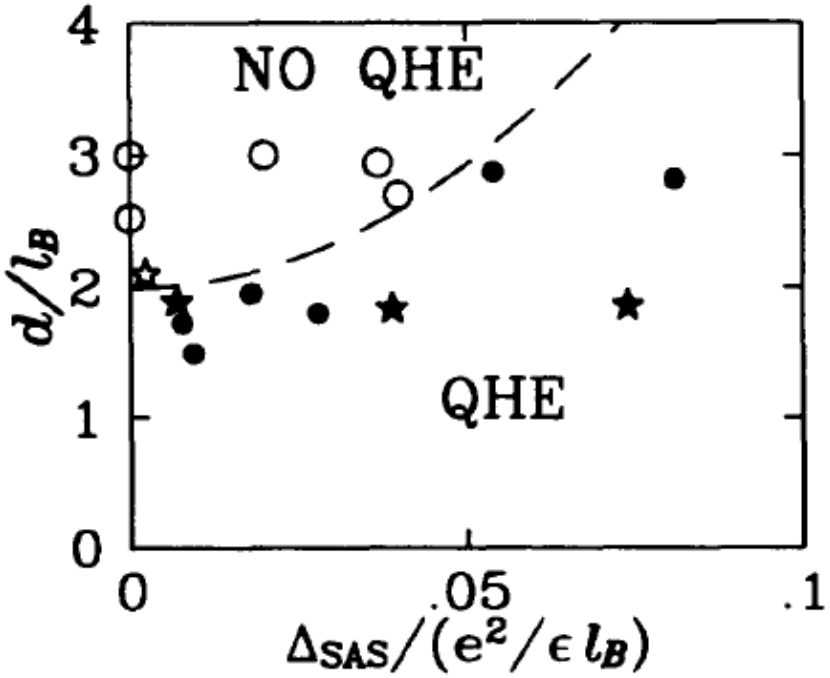

Fertig (1989); MacDonald et al. (1990); L. Brey and H. Fertig (2000)

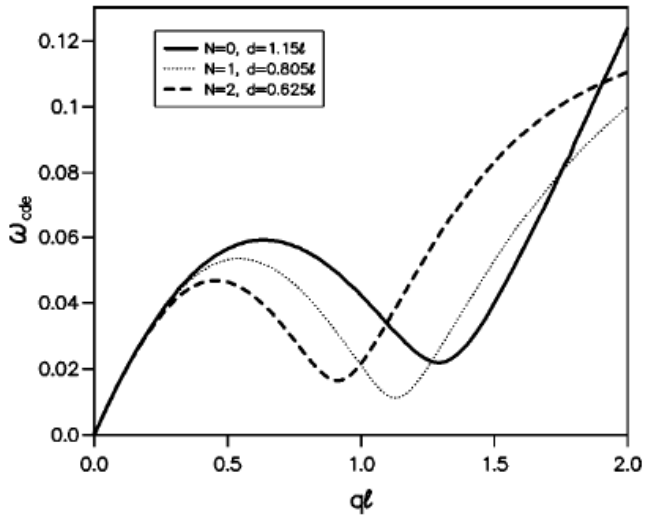

Roton spectrum in pancake polar condensates

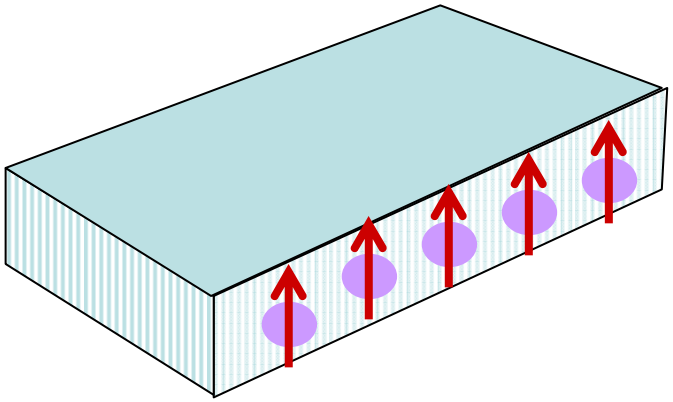

Santos, Shlyapnikov, Lewenstein (2000)
Fischer (2006)

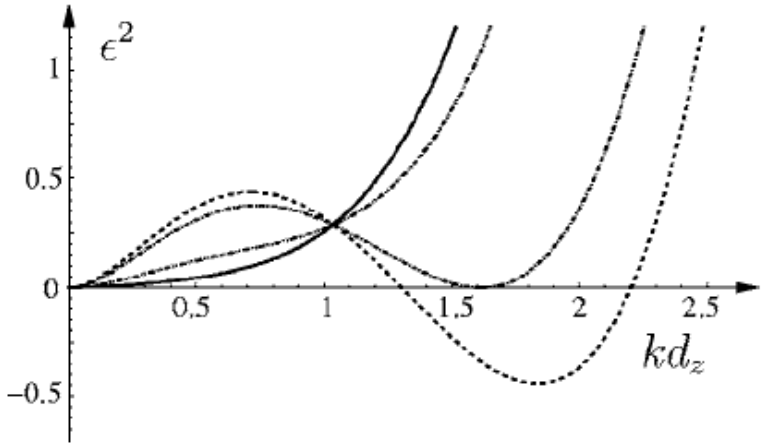

Origin of roton softening

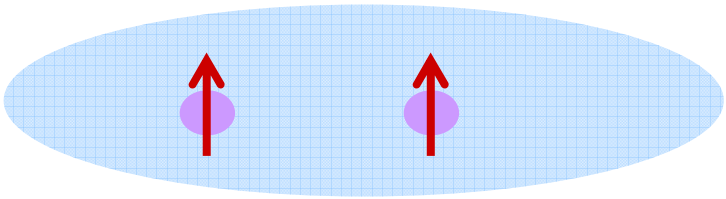

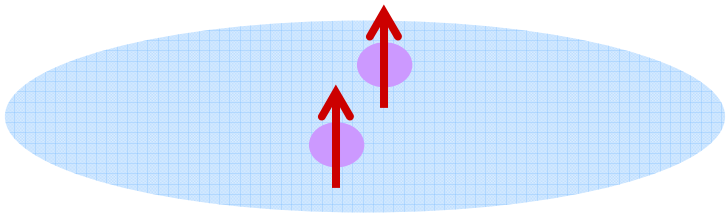

Repulsion at long distances

Attraction at short distances

Stability of the supersolid phase is a subject of debate

Magnetic dipolar interactions in ultracold atoms

Magnetic dipolar interactions in spinor condensates

$$U_{\text{contact}}(\mathbf{r}) = \frac{4\pi\hbar^2 a}{m}\delta(\mathbf{r}) \qquad V_{\text{dd}} = \frac{\mu_0\mu^2}{4\pi\, r^3}\left(1 - 3\cos^2\theta\right)$$

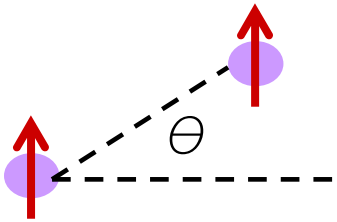

Comparison of contact and dipolar interactions.
Typical value a=100a_B

$$\epsilon = \frac{\mu_0\mu^2 m}{12\pi\hbar^2 a}$$

For ^{87}Rb $\mu=\mu_B$ and ϵ=0.007

For ^{52}Cr $\mu=6\mu_B$ and ϵ=0.16

Bose condensation of ^{52}Cr.
T. Pfau et al. (2005)

Review:
Menotti et al.,
arXiv 0711.3422

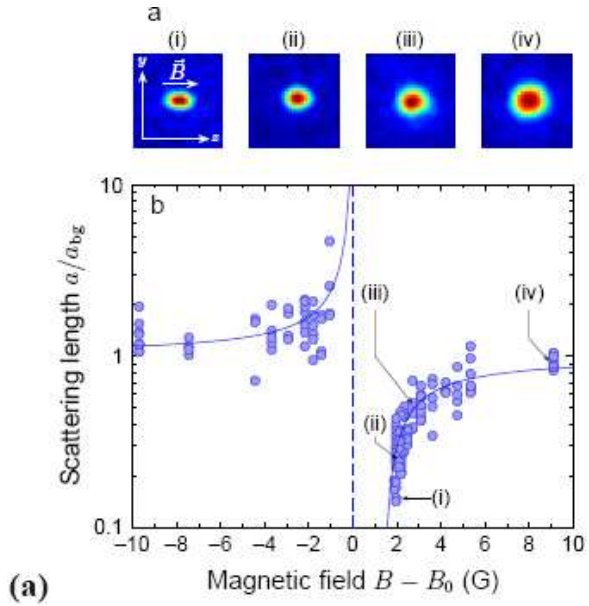

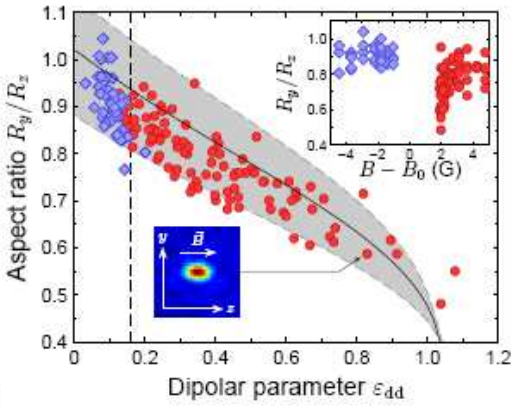

Magnetic dipolar interactions in spinor condensates

Interaction of F=1 atoms

$$V_S = c_0 + c_2 \vec{f}_1 \cdot \vec{f}_2$$

$$c_2 \equiv (4\pi\hbar^2/M) \times (a_2 - a_0)/3$$

Ferromagnetic Interactions for ^{87}Rb

a_2-a_0= -1.07 a_B

A. Widera, I. Bloch et al.,
New J. Phys. 8:152 (2006)

Spin-depenent part of the interaction is small.
Dipolar interaction may be important (D. Stamper-Kurn)

Spontaneously modulated textures in spinor condensates

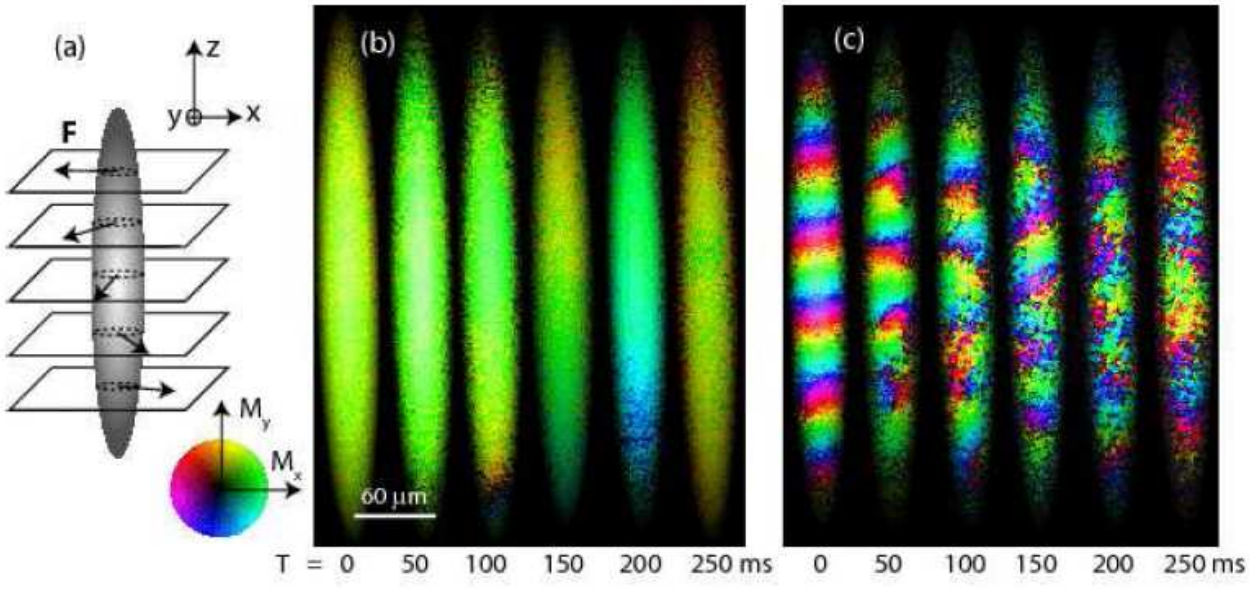

Vengalattore et al.
PRL (2008)

Fourier spectrum of the fragmented condensate

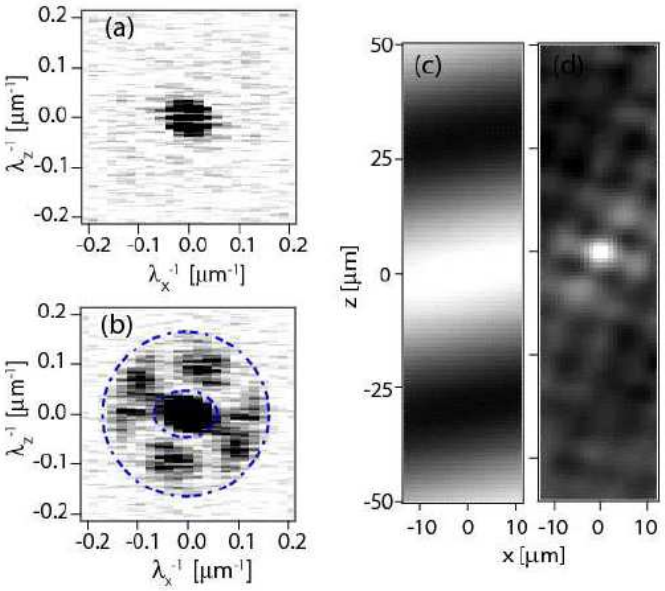

Patterns due to magnetic dipolar interactions

C. Kittel, Rev. Mod. Phys. (1949)

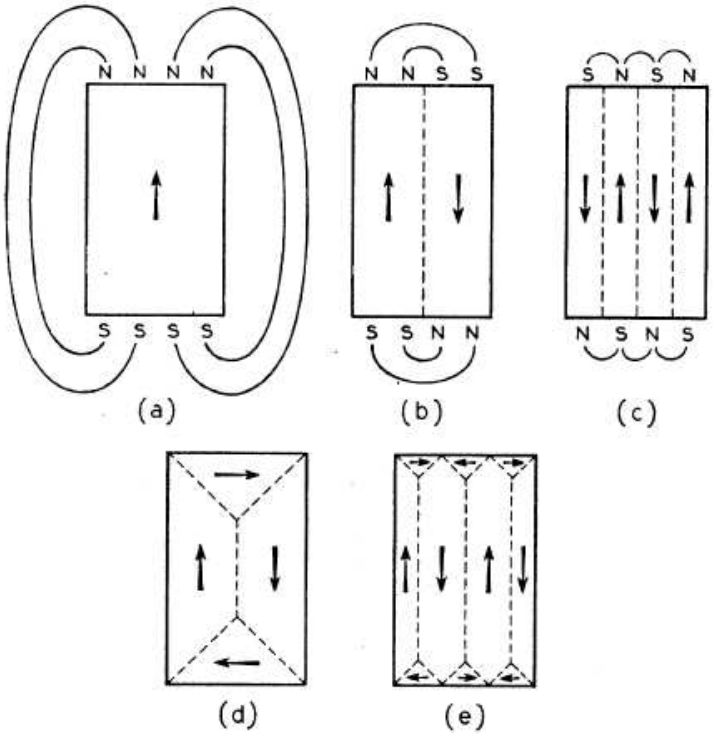

In the context of cold atoms see
P. Meystre et al. Phys. Rev. A (2002)

Typical patterns due to dipolar interactions: 1d structures

Vengalattore et al. PRL (2008)

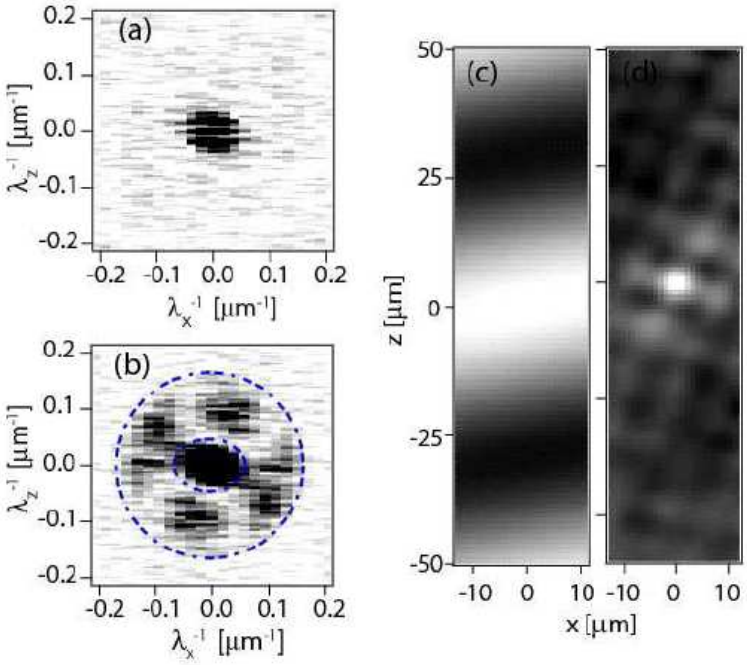

Berkeley experiments:
2D structures

Energy scales

Magnetic Field

- Larmor Precession (100 kHz)
- Quadratic Zeeman (0-20 Hz)

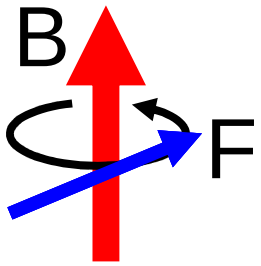

S-wave Scattering

- Spin independent ($g_0 n$ = kHz)
- Spin dependent ($g_s n$ = 10 Hz)

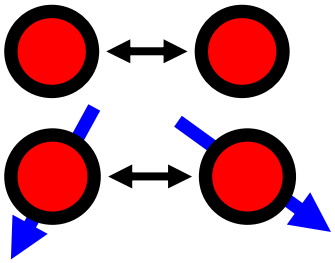

Dipolar Interaction

- Anisotropic ($g_d n$=10 Hz)
- Long-ranged

Reduced Dimensionality

- Quasi-2D geometry

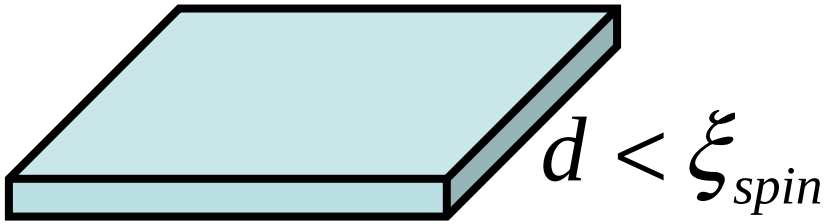

Dipolar interactions

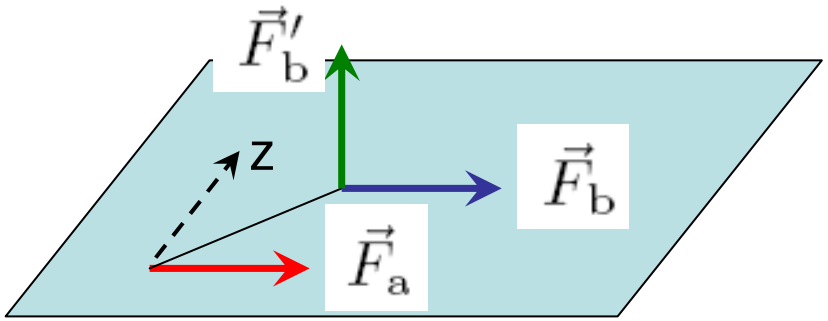

Static interaction

$\vec{F}_{\mathrm{b}}$ parallel to $\vec{F}_{\mathrm{a}}$ is preferred

"Head to tail" component dominates

Averaging over Larmor precession

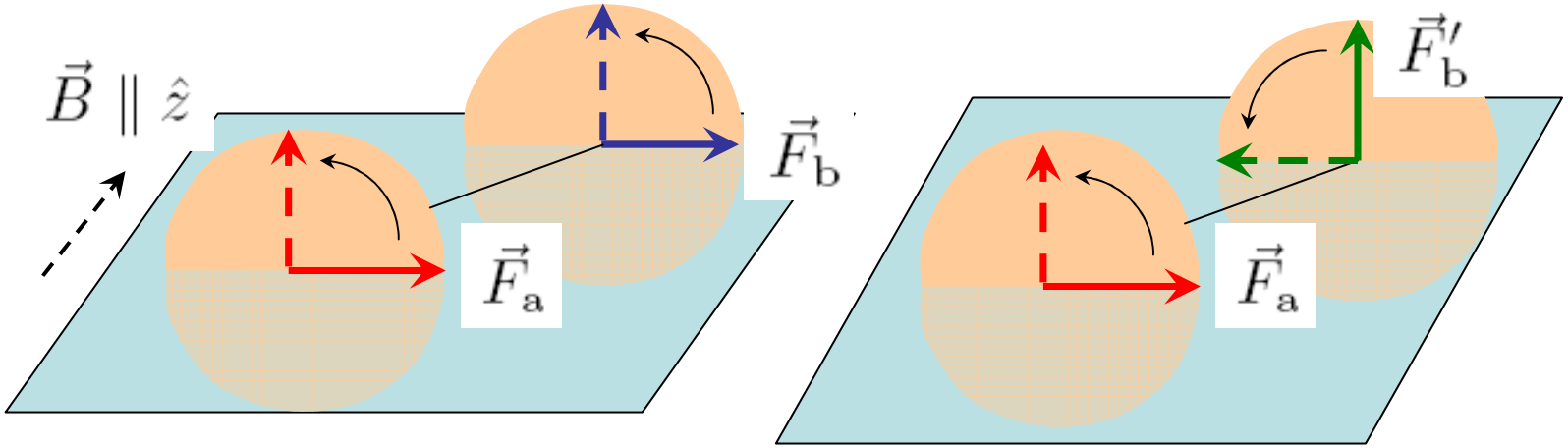

$\vec{F}'_{\mathrm{b}}$ perpendicular to $\vec{F}_{\mathrm{a}}$ is preferred. "Head to tail" component is averaged with the "side by side"

Instabilities: qualitative picture

Stability of systems with static dipolar interactions

Ferromagnetic configuration is robust against small perturbations. Any rotation of the spins conflicts with the “head to tail” arrangement

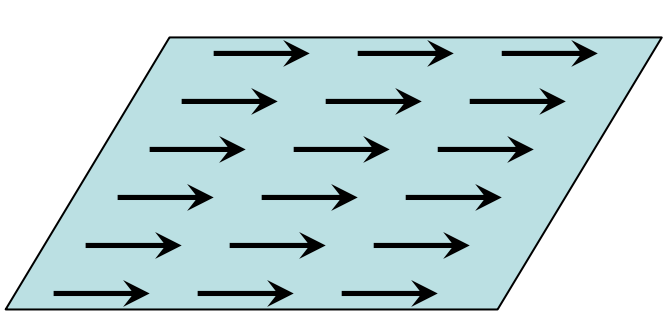

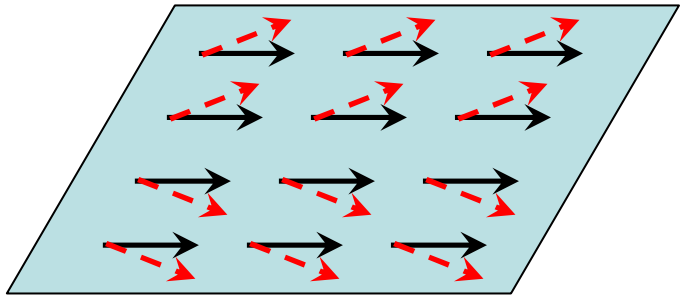

Large fluctuation required to reach a lower energy configuration

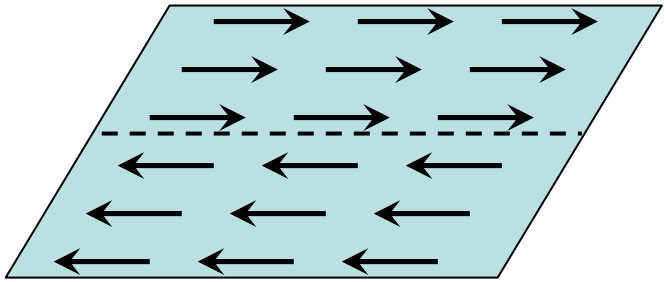

Dipolar interaction averaged after precession

"Head to tail" order of the transverse spin components is violated by precession. Only need to check whether spins are parallel

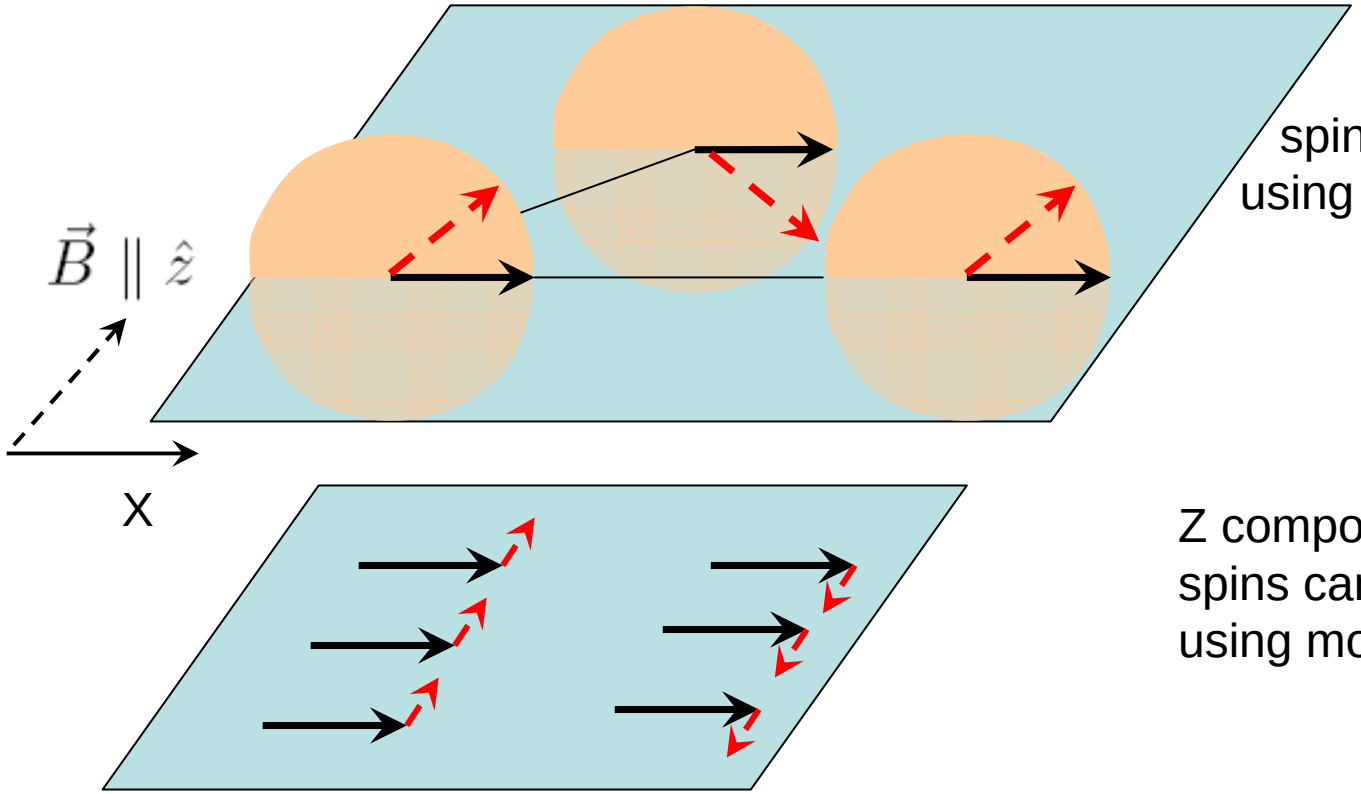

XY components of the spins can lower the energy using modulation along z.

Z components of the spins can lower the energy using modulation along x

Strong instabilities of systems with dipolar interactions after averaging over precession

Instabilities: technical details

From Spinless to Spinor Condensates

$$\langle \Psi \rangle = \sqrt{n} e^{i\phi} \qquad \langle \Psi \rangle = \sqrt{n}\left[\Phi_x, \Phi_y, \Phi_z\right]$$

$$\Psi = \sqrt{n}\begin{bmatrix} ie^{i\eta+i\eta_\perp}\cos(\phi+i\chi)\frac{\sin(\rho)}{\sqrt{\cosh(2\chi)}} \\ ie^{i\eta+i\eta_\perp}\sin(\phi+i\chi)\frac{\sin(\rho)}{\sqrt{\cosh(2\chi)}} \\ e^{i\eta}\cos(\rho) \end{bmatrix}$$

Charge mode:

n is density and η is the overall phase

Spin mode:

ϕ determines spin orientation in the XY plane

χ determines longitudinal magnetization (Z-component)

Hamiltonian

Quasi-2D

Magnetic Field

$$\mathcal{H} = \int d^3x \Psi_x^\dagger \left[-\frac{\nabla^2}{2m} - \mu + \frac{1}{2}\omega_n^2 \left(\hat{n}\cdot\vec{x}\right)^2 + \left(-p + B_0\right)\left(\hat{B}\cdot\vec{F}\right) + q\left(\hat{B}\cdot\vec{F}\right)^2 \right] \Psi_x$$

$$+ \int d^3x d^3x' \frac{1}{2} g_{3D}^{\mu\nu}(x - x') : (\Psi_x^\dagger F^\mu \Psi_x)(\Psi_{x'}^\dagger F^\nu \Psi_{x'}) :$$

Dipolar Interaction

$$g_{3D}^{ij}(\Delta x) = -g_s \delta^{ij}\delta(\Delta x) + g_d \frac{1}{|\Delta x|^3}\left[\delta^{ij} - 3\Delta\hat{x}^i \Delta\hat{x}^j\right]$$

S-wave Scattering

$$g_{3D}^{00}(\Delta x) = (g_0 + g_s)\delta(\Delta x)$$

$$(F^0)_{jk} = \delta_{jk}$$

$$(F^i)_{jk} = -i\epsilon_{ijk}$$

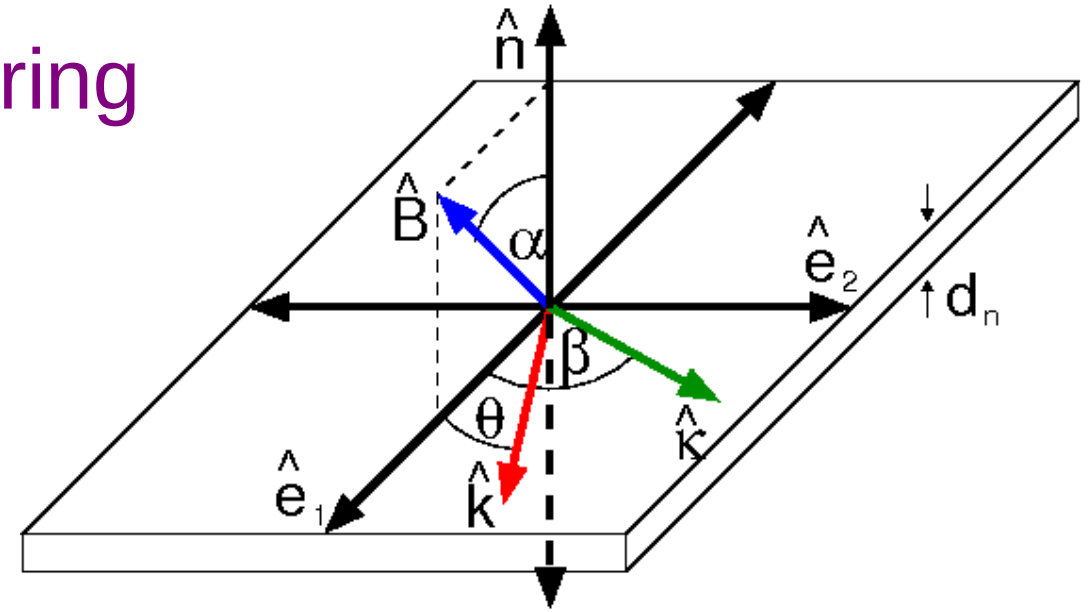

Precessional and Quasi-2D Averaging

Rotating Frame

$$\Psi \rightarrow R(t,x)\Psi$$

$$R(t,x) = \exp\left[i(B_0 t + \vec{\kappa}\cdot\vec{x})\hat{B}\cdot\vec{F}\right]$$

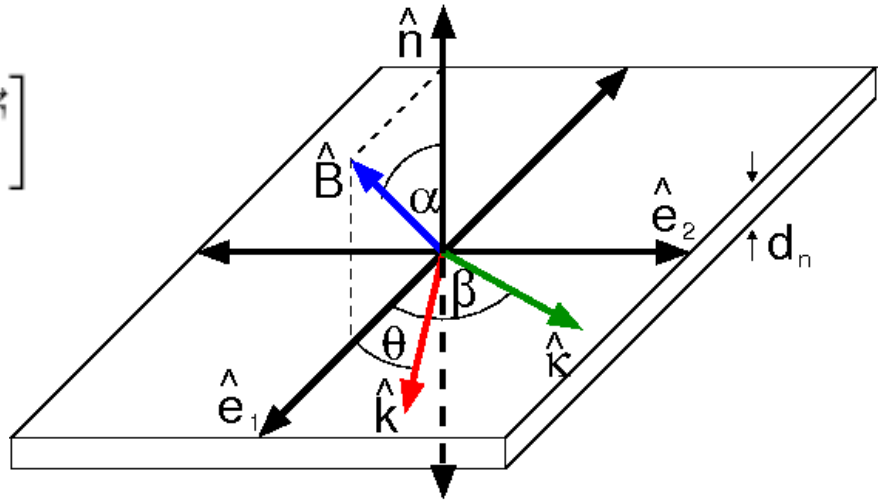

Gaussian Profile

$$\Psi(x_1\hat{e}_1 + x_1\hat{e}_2 + x_n\hat{n}) =$$

$$\frac{e^{-x_n^2/4d_n^2}}{(2\pi d_n^2)^{1/4}}\Psi(x_1\hat{e}_1 + x_2\hat{e}_2)$$

Quasi-2D Time Averaged Dipolar Interaction

$$\left(\delta^{ij} - 3\Delta\hat{x}^i\Delta\hat{x}^j\right) \rightarrow \int_{-\infty}^{\infty}\frac{d(\hat{n}\cdot\Delta\vec{x})}{2\sqrt{\pi}d_n}e^{-(\hat{n}\cdot\Delta\vec{x})^2/4d_n^2}\int_{-\pi/B_0}^{\pi/B_0}B_0 dt$$

$$\left[R(t,x)^T_{ii'}\left(\delta^{i'j'} - 3\Delta\hat{x}^{i'}\Delta\hat{x}^{j'}\right)R(t,x')_{j'j}\right]$$

Collective Modes

Mean Field

$$\Psi = \Psi_0 + \delta\Psi$$

Collective Fluctuations
(Spin, Charge)

Equations of Motion

$$i\partial_t \begin{bmatrix} \delta\Psi_k \\ \delta\Psi^*_{-k} \end{bmatrix} = \begin{bmatrix} M_k & N_k \\ -N^*_{-k} & -M^*_{-k} \end{bmatrix} \begin{bmatrix} \delta\Psi_k \\ \delta\Psi^*_{-k} \end{bmatrix}$$

$$\delta\Psi(x,t) \sim \exp(i\omega_k - ikx)$$

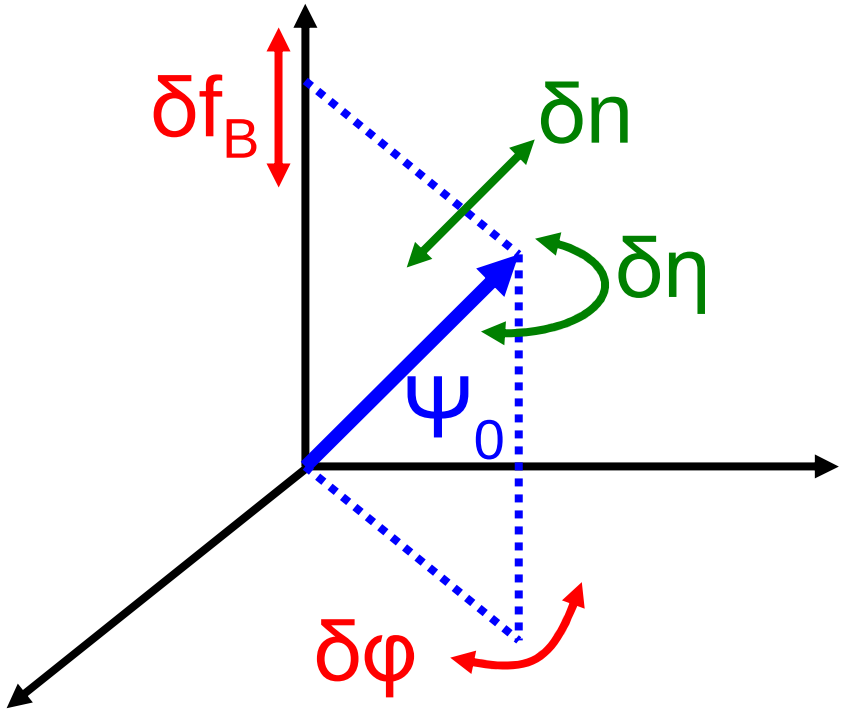

Spin Mode

δf_B – longitudinal magnetization
δφ – transverse orientation

Charge Mode

δn – 2D density

δη – global phase

Instabilities of collective modes

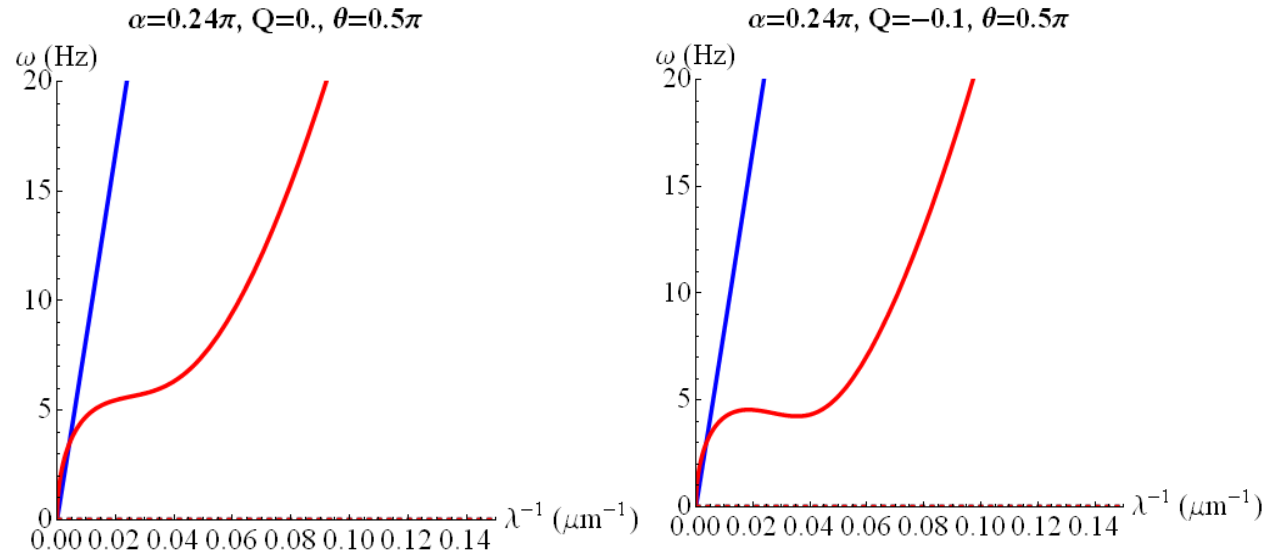

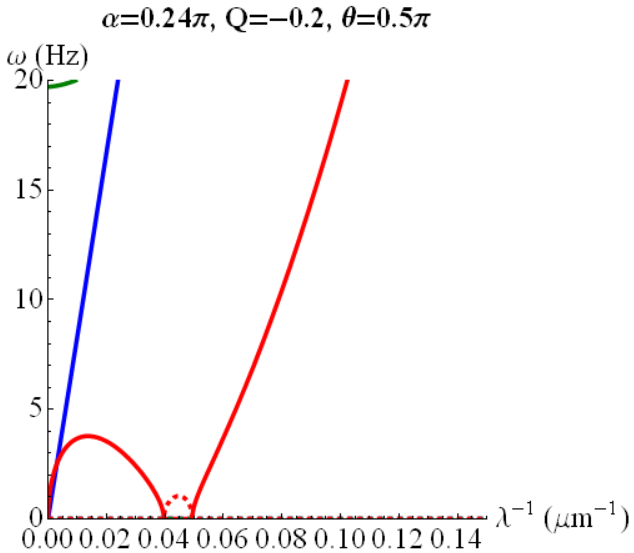

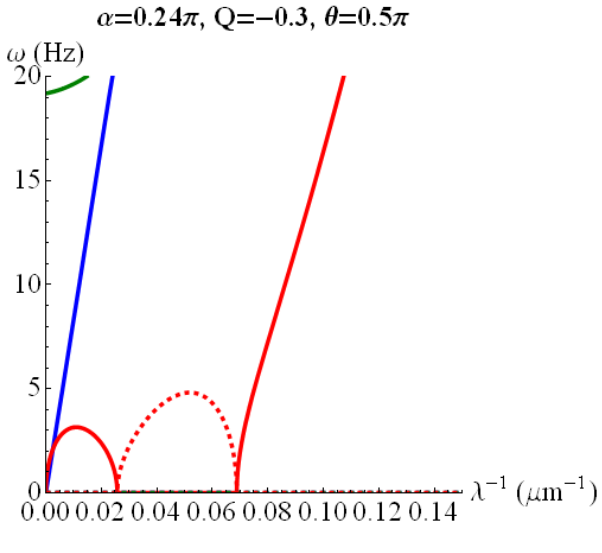

Q measures the strength of quadratic Zeeman effect

$$Q = -\frac{q}{2g^{\perp}n_{2D}}$$

Instabilities of collective modes

Wide range of instabilities tuned by quadratic Zeeman, AC Stark shift, initial spiral spin winding

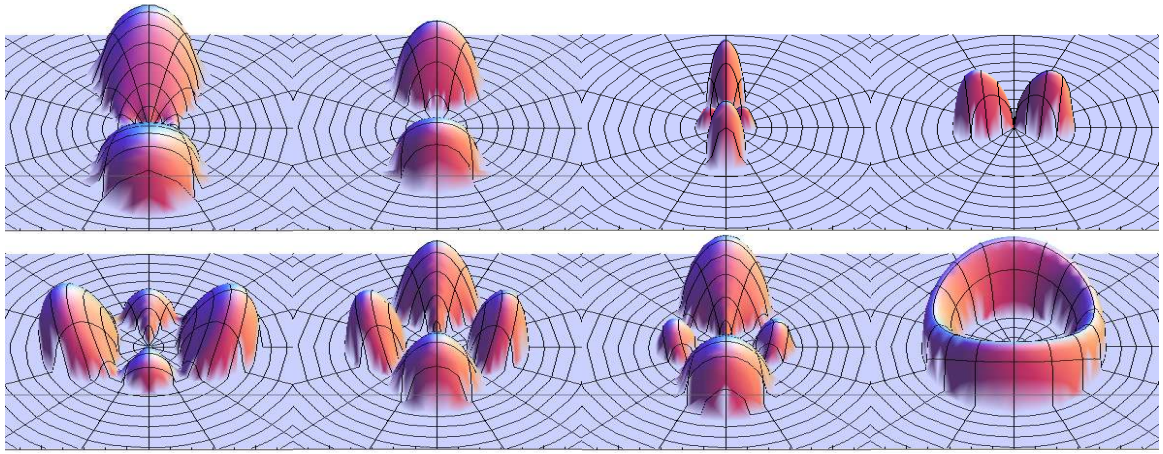

Unstable modes in the regime corresponding to Berkeley experiments

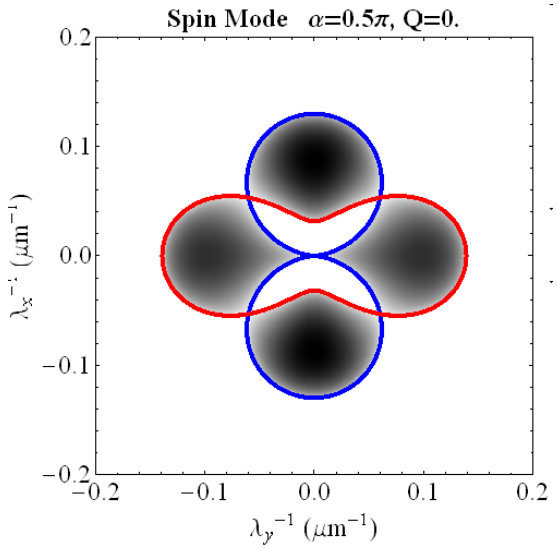

Results of Berkeley experiments

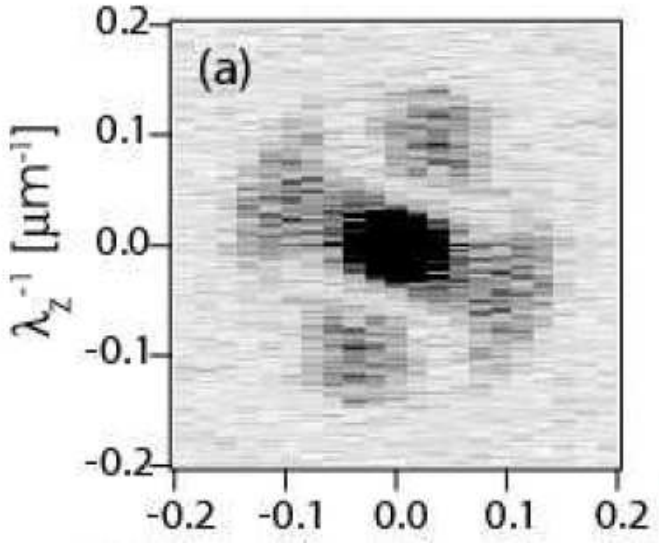

Instabilities of collective modes

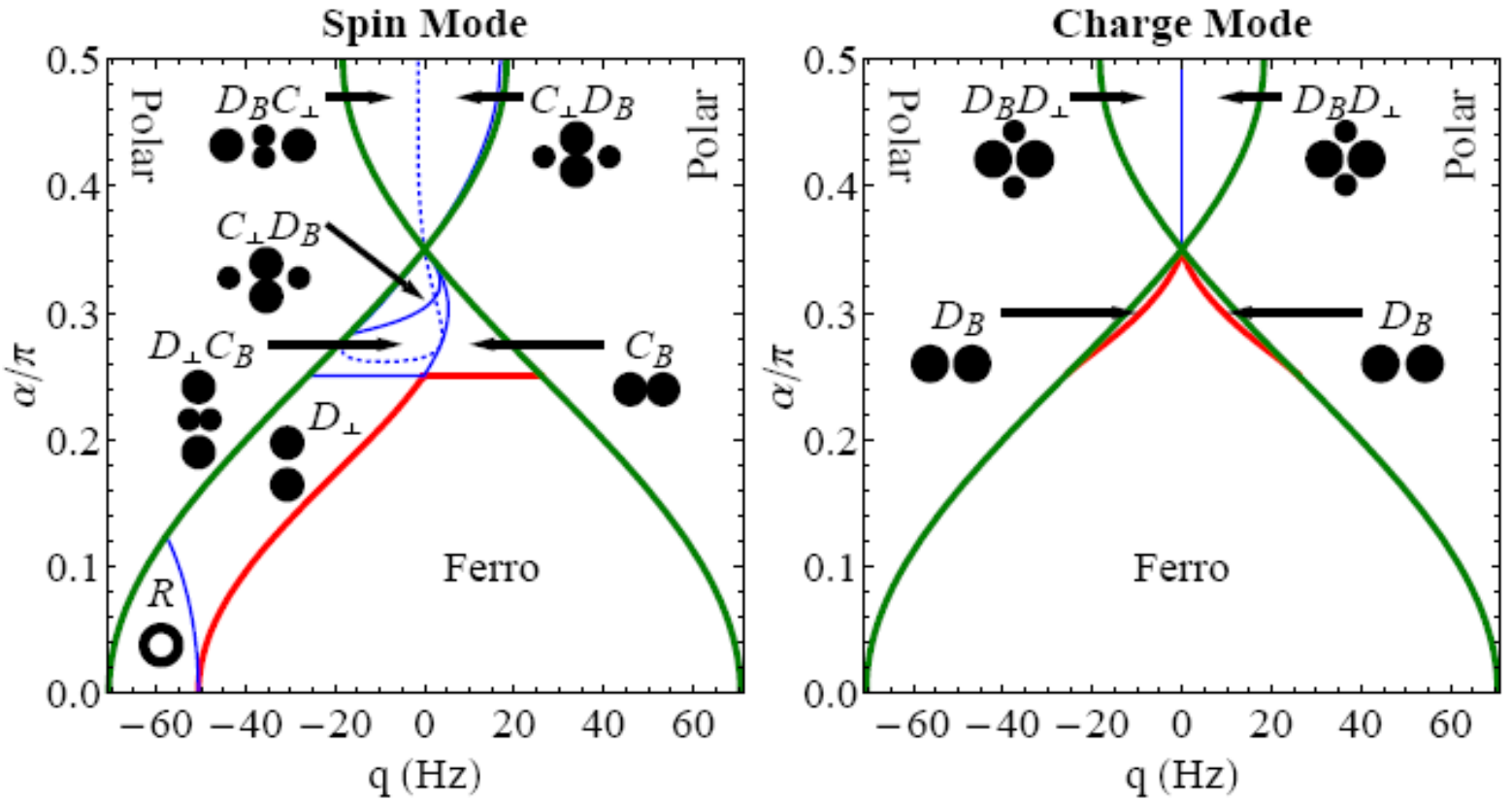

Many-body decoherence and Ramsey interferometry

Collaboration with A. Widera, S. Trotzky, P. Cheinet, S. Fölling, F. Gerbier, I. Bloch, V. Gritsev, M. Lukin

Phys. Rev. Lett. 100:140401 (2008)

Ramsey interference

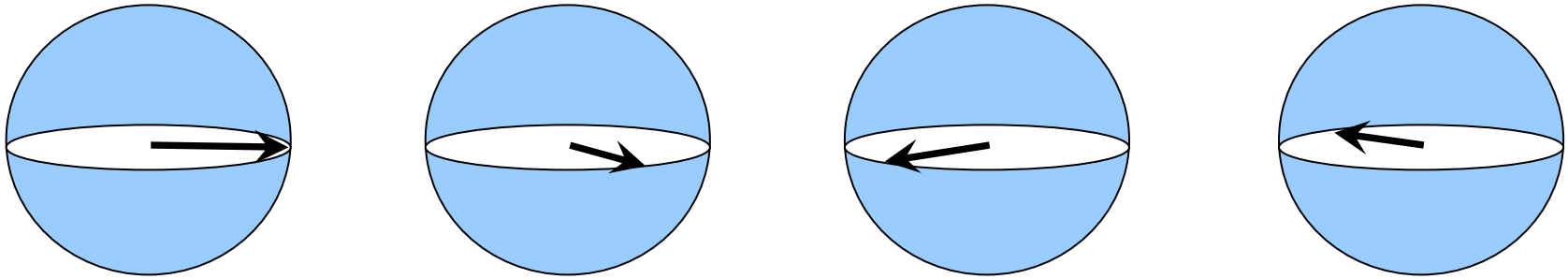

$$|\Psi\rangle = e^{-iE_1 t}|\uparrow\rangle + e^{-iE_2 t}|\downarrow\rangle$$

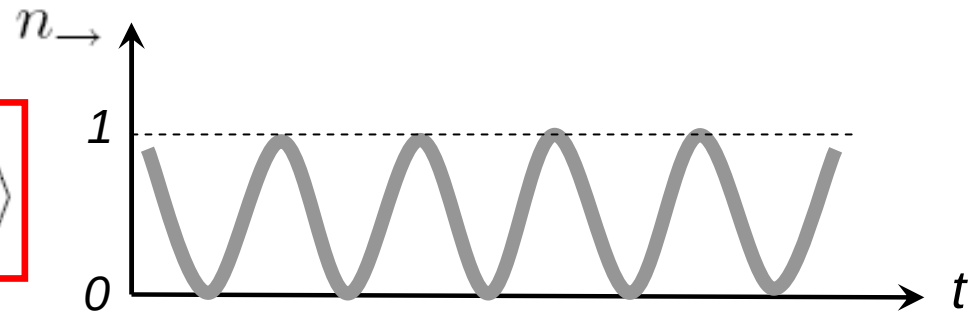

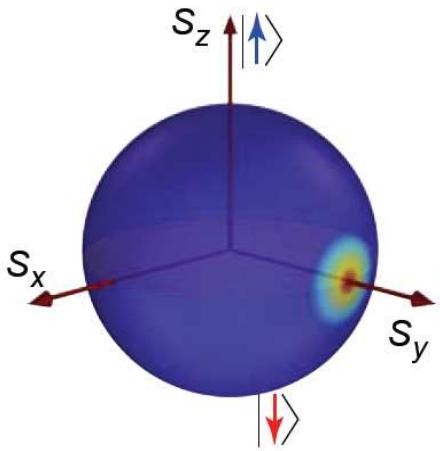

Working with *N* atoms improves the precision by $\sqrt{N}$.
Need spin squeezed states to improve frequency spectroscopy

Squeezed spin states for spectroscopy

Motivation: improved spectroscopy, e.g. Wineland et. al. PRA 50:67 (1994)

Generation of spin squeezing using interactions.
Two component BEC. Single mode approximation

$$\mathcal{H} = \chi_s \left(S^z_{\rm tot}\right)^2$$

Kitagawa, Ueda, PRA 47:5138 (1993)

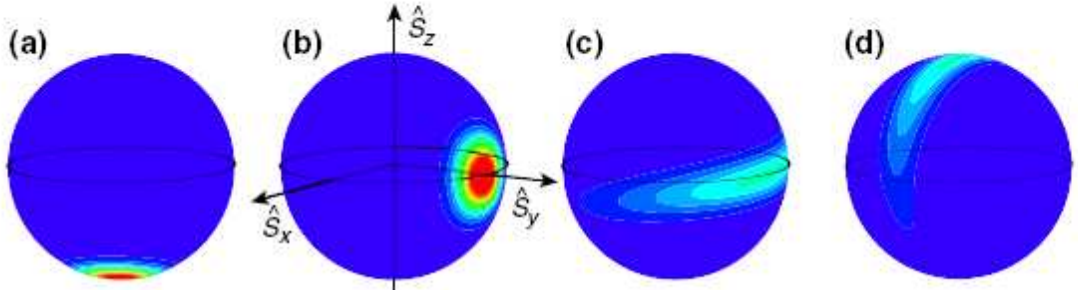

$$\mathcal{H} = \int dx \left[g_c \left(n_1 + n_2\right)^2 + g_s (n_1 - n_2)^2 + \frac{|\nabla \Psi_1|^2}{2m} + \frac{|\nabla \Psi_2|^2}{2m} \right]$$

In the single mode approximation we can neglect kinetic energy terms

$$\mathcal{H}_{\rm SMA} = \frac{g_s}{V} \left(N_1 - N_2\right)^2$$

Interaction induced collapse of Ramsey fringes

Ramsey fringe visibility

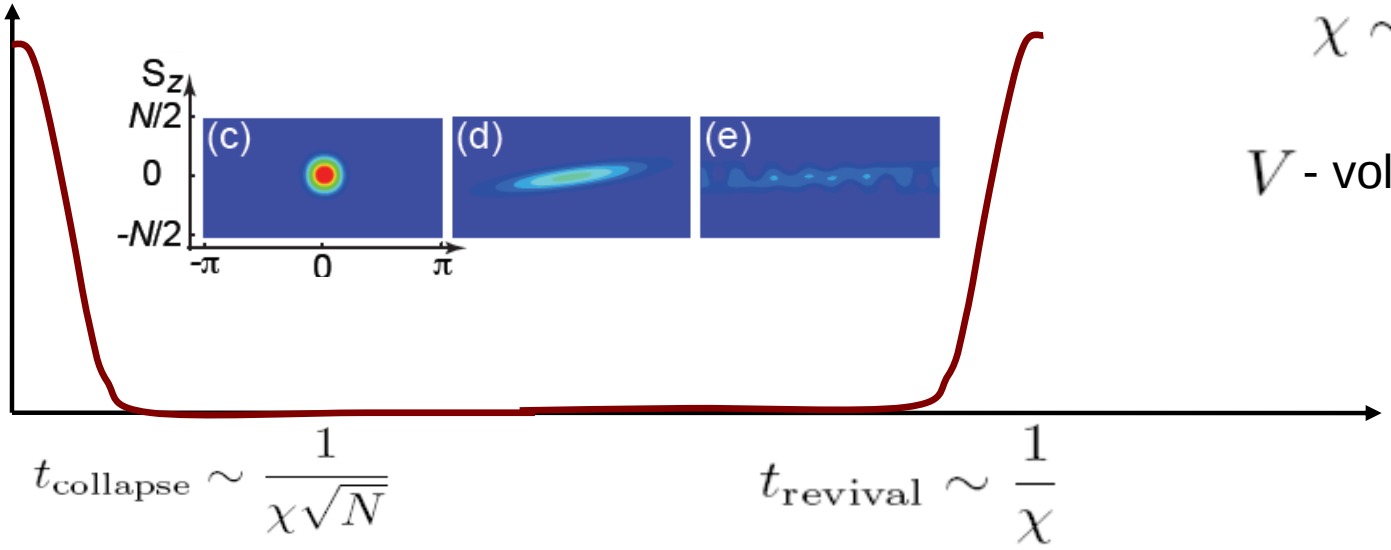

$$\chi \sim \frac{\hbar^2 a_s}{M V}$$

V - volume of the system

$$t_{\mathrm{collapse}} \sim \frac{1}{\chi\sqrt{N}}$$

$$t_{\mathrm{revival}} \sim \frac{1}{\chi}$$

Experiments in 1d tubes:

A. Widera, I. Bloch et al.

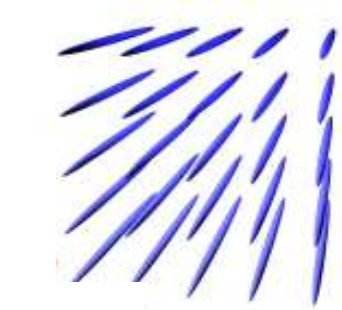

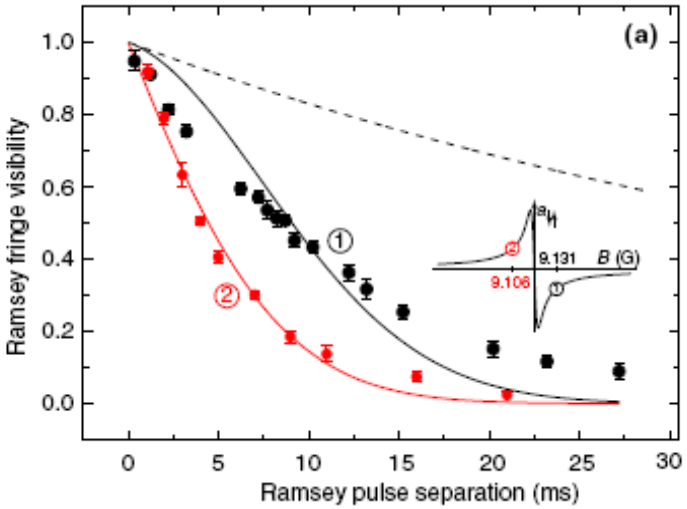

Spin echo. Time reversal experiments

Single mode approximation

$$\mathcal{H}_{\mathrm{SMA}} = \frac{g_s}{V}\left(N_1 - N_2\right)^2$$

$$g_s = \frac{g_{11} - g_{12}}{2}$$

The Hamiltonian can be reversed by changing a_{12}

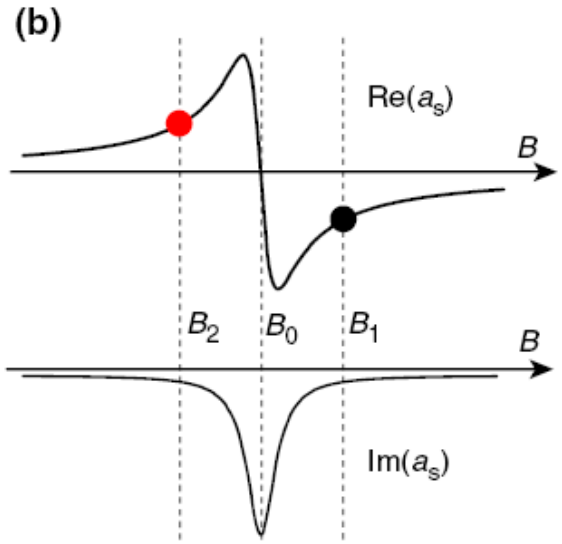

$$a_s \rightarrow -a_s$$

$$\mathcal{H}_{\mathrm{SMA}} \rightarrow -\mathcal{H}_{\mathrm{SMA}}$$

$$e^{i\int_T^{2T}\mathcal{H}_{\mathrm{SMA}}(t)dt} \times e^{i\int_0^{T}\mathcal{H}_{\mathrm{SMA}}(t)dt} = 1$$

Predicts perfect spin echo

Spin echo. Time reversal experiments

Expts: A. Widera, I. Bloch et al.

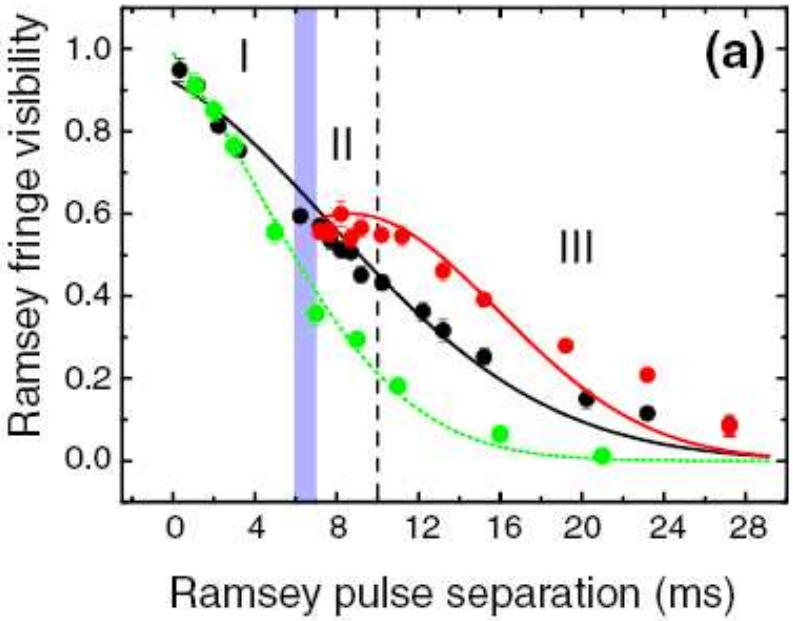

No revival?

$$a_s \longrightarrow -a_s$$

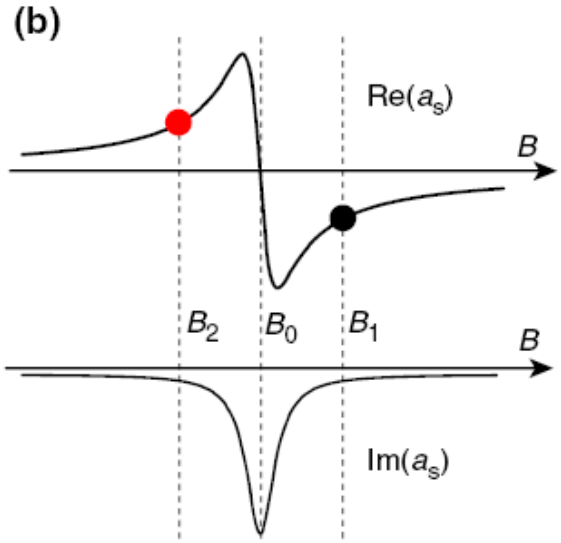

Experiments done in array of tubes.
Strong fluctuations in 1d systems.
Single mode approximation does not apply.
Need to analyze the full model

$$\mathcal{H} = \int dx \left[g_c\,(n_1+n_2)^2 + g_s(n_1-n_2)^2 + \frac{|\nabla\Psi_1|^2}{2m} + \frac{|\nabla\Psi_2|^2}{2m} \right]$$

Interaction induced collapse of Ramsey fringes. Multimode analysis

Low energy effective theory: Luttinger liquid approach

Luttinger model

$$S^+(x,t) \sim e^{i\phi_s(x,t)} \qquad [S^z(x), \phi_s(x')] = -i\delta(x-x')$$

$$\mathcal{H}_s = \int_0^L dx \left[g_s (S^z)^2 + \frac{\rho}{2m} (\nabla \phi_s)^2 \right]$$

Changing the sign of the interaction reverses the interaction part of the Hamiltonian but not the kinetic energy

$$\mathcal{H}_s = \sum_q \left[g_s(t) S^z_q S^{z*}_q + \frac{\rho\, q^2}{m} \phi_{sq} \phi^*_{sq} \right]$$

$$\left[S^z_{q'}, \phi_{sq} \right] = -i\delta_{qq'}$$

Time dependent harmonic oscillators can be analyzed exactly

Time-dependent harmonic oscillator

$$\mathcal{H} = \frac{p^2}{2m(t)} + k\,\frac{q^2}{2}$$

See e.g. Lewis, Riesengeld (1969)
Malkin, Man'ko (1970)

Explicit quantum mechanical wavefunction can be found

$$\psi(p,t) = \frac{\Phi(\frac{p}{c(t)})}{\sqrt{c(t)}}\, e^{i\alpha(t)p^2 + i\gamma(t)}$$

From the solution of classical problem

$$\ddot{c} + \omega^2(t)\, c = \frac{\omega_0^2}{c^3}$$

We solve this problem for each momentum component

$$\mathcal{H}_s = \sum_q \left[g_s(t) S_q^z S_q^{z*} + \frac{\rho\, q^2}{m} \phi_{sq} \phi_{sq}^* \right]$$

Interaction induced collapse of Ramsey fringes in one dimensional systems

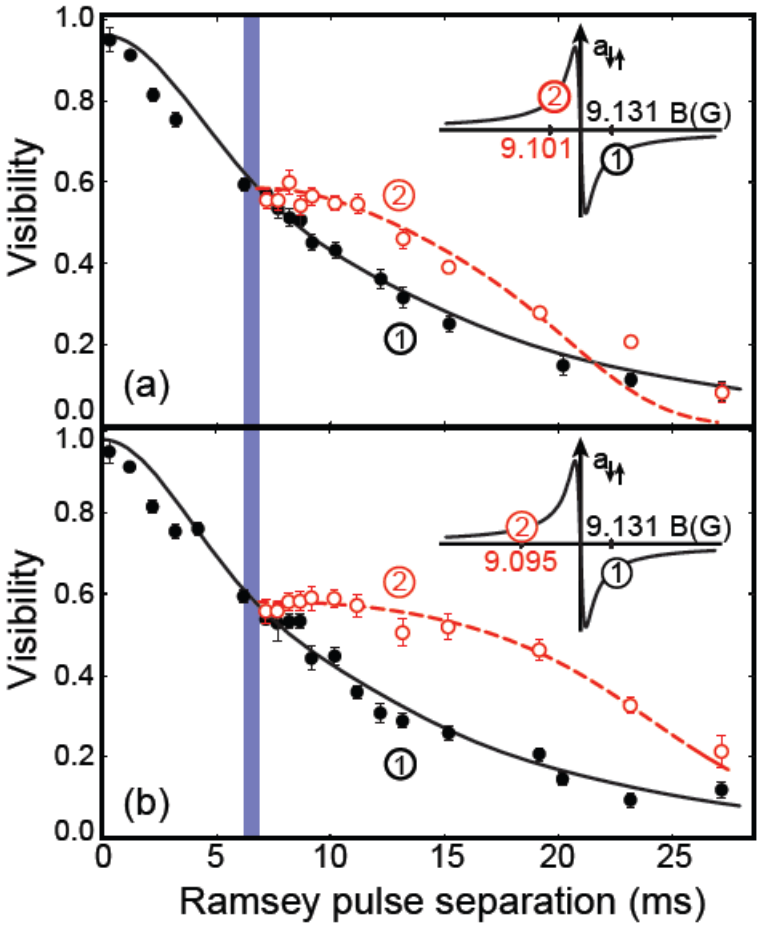

Only q=0 mode shows complete spin echo
Finite q modes continue decay

The net visibility is a result of competition between q=0 and other modes

Conceptually similar to experiments with dynamics of split condensates.
T. Schumm's talk

Fundamental limit on Ramsey interferometry

Superexchange interaction in experiments with double wells

Refs:

Theory: A.M. Rey et al., Phys. Rev. Lett. 99:140601 (2007)
Experiment: S. Trotzky et al., Science 319:295 (2008)

Two component Bose mixture in optical lattice

Example: $^{87}\mathrm{Rb}$. Mandel et al., Nature 425:937 (2003)

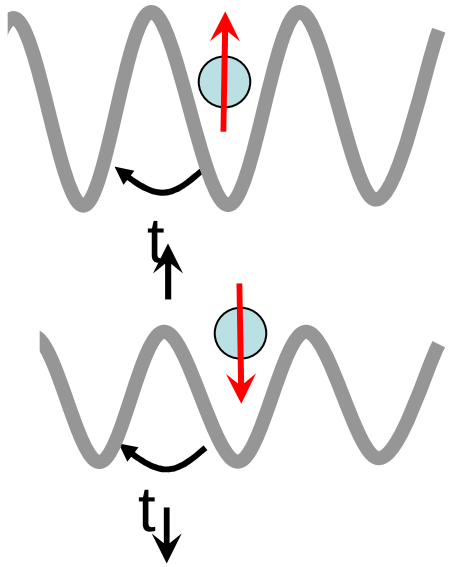

$$|\uparrow\rangle = |F=1, m_F=-1\rangle$$

$$|\downarrow\rangle = |F=2, m_F=-2\rangle$$

Two component Bose Hubbard model

$$\mathcal{H} = -\ t_\uparrow \sum_{\langle ij\rangle} b^\dagger_{i\uparrow} b_{j\uparrow} - t_\downarrow \sum_{\langle ij\rangle} b^\dagger_{i\downarrow} b_{j\downarrow} + U_{\uparrow\uparrow} \sum_i n_{i\uparrow}(n_\uparrow - 1)$$

$$+\ U_{\downarrow\downarrow} \sum_i n_{i\downarrow}(n_\downarrow - 1) + U_{\uparrow\downarrow} \sum_i n_{i\uparrow} n_\downarrow$$

Quantum magnetism of bosons in optical lattices

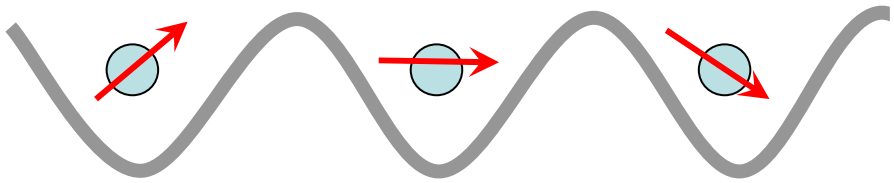

Duan, Demler, Lukin, PRL 91:94514 (2003)
Altman et al., NJP 5:113 (2003)

$$\mathcal{H} = J_z \sum_{\langle ij \rangle} \sigma_i^z \sigma_j^z + J_\perp \sum_{\langle ij \rangle} \left(\sigma_i^x \sigma_j^x + \sigma_i^y \sigma_j^y \right)$$

$$J_z = \frac{t_\uparrow^2 + t_\downarrow^2}{2U_{\uparrow\downarrow}} - \frac{t_\uparrow^2}{U_{\uparrow\uparrow}} - \frac{t_\downarrow^2}{U_{\downarrow\downarrow}} \qquad J_\perp = -\frac{t_\uparrow t_\downarrow}{U_{\uparrow\downarrow}}$$

- Ferromagnetic $U_{\uparrow\downarrow} >> U_{\uparrow\uparrow},\ U_{\downarrow\downarrow}$
- Antiferromagnetic $U_{\uparrow\downarrow} << U_{\uparrow\uparrow},\ U_{\downarrow\downarrow}$

Observation of superexchange in a double well potential

Theory: A.M. Rey et al., PRL (2007)

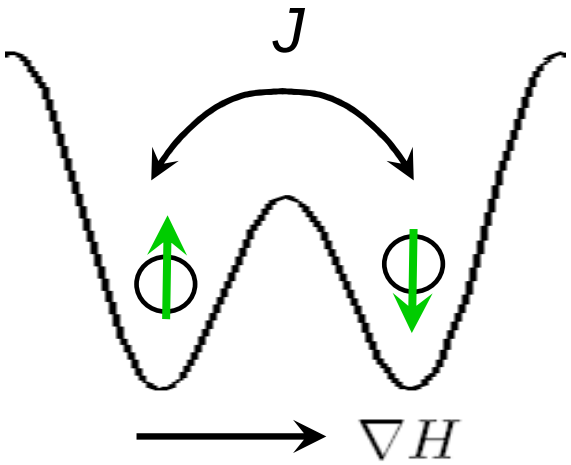

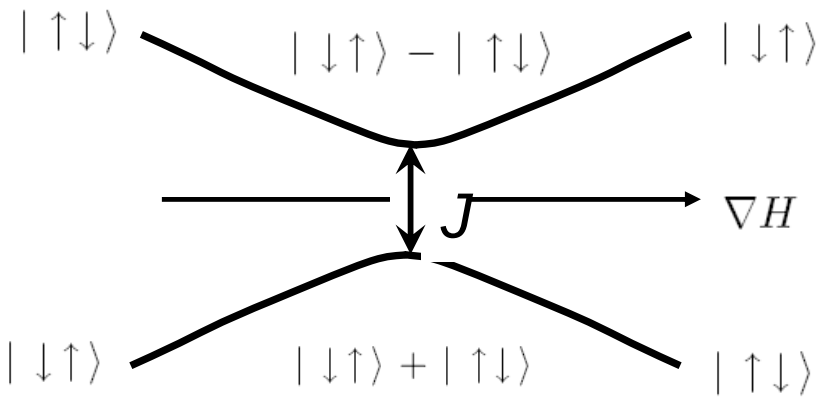

Use magnetic field gradient to prepare a state $|\downarrow\uparrow\rangle$

Observe oscillations between $|\downarrow\uparrow\rangle$ and $|\uparrow\downarrow\rangle$ states

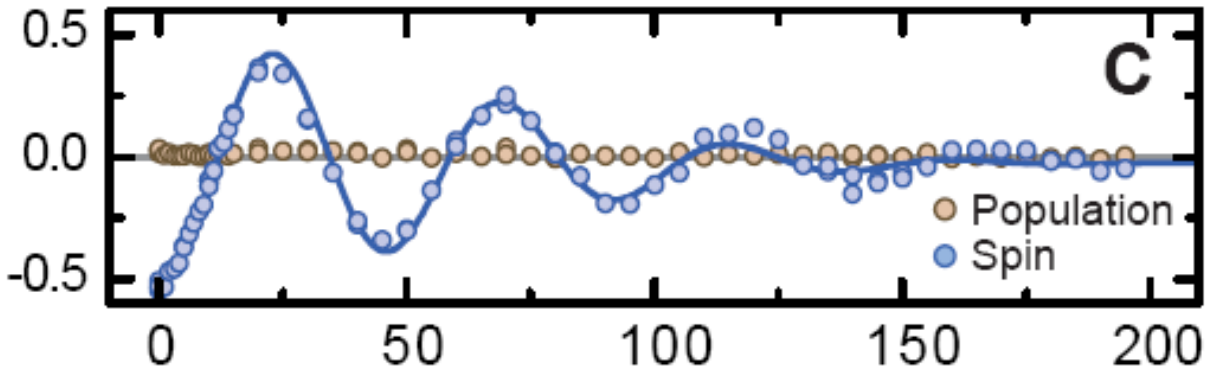

Experiment:
Trotzky et al.,
Science (2008)

Preparation and detection of Mott states of atoms in a double well potential

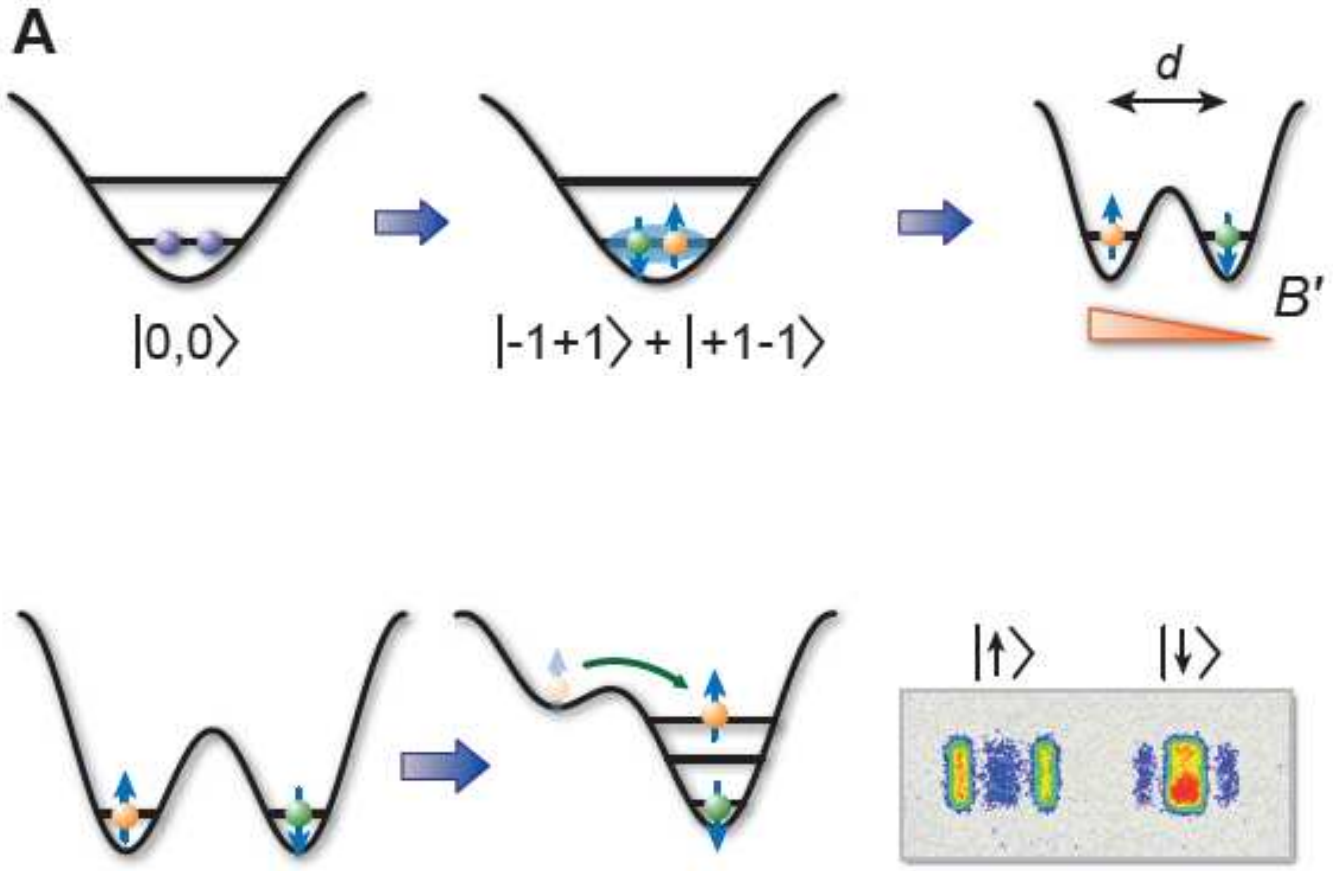

Comparison to the Hubbard model

Experiments: I. Bloch et al.

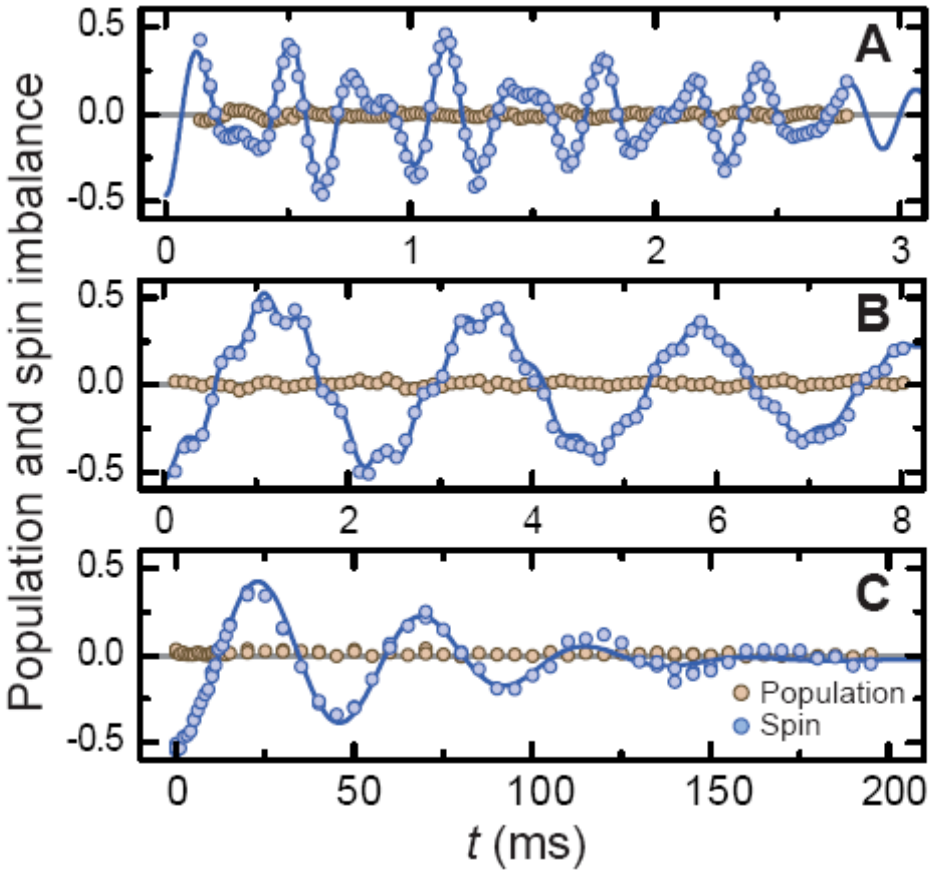

$$\hbar\omega_{1,2} = \frac{U}{2}\left(\sqrt{\left(\frac{4J}{U}\right)^2 + 1} \pm 1\right)$$

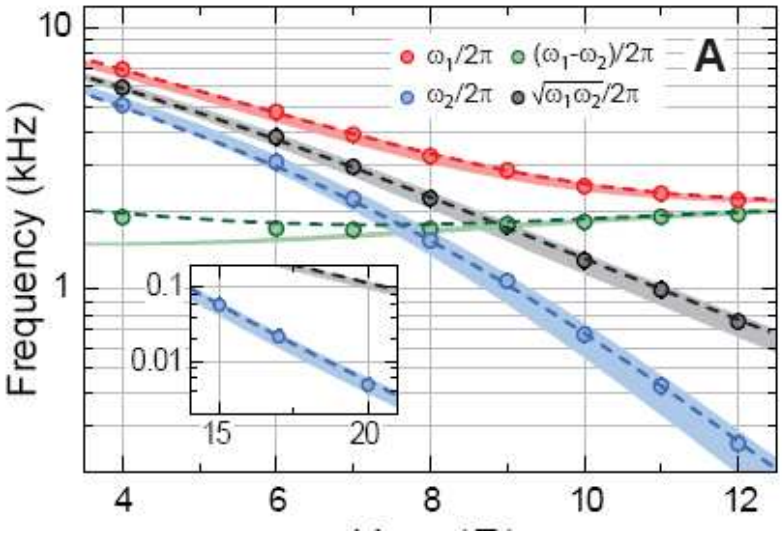

Beyond the basic Hubbard model

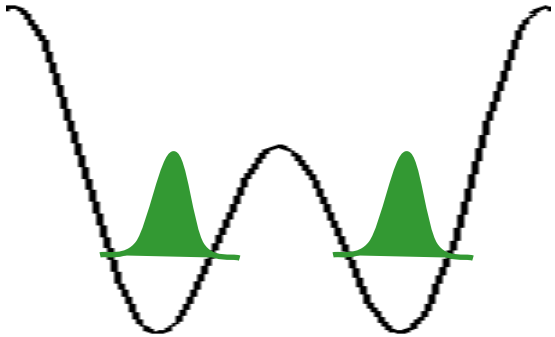

Basic Hubbard model includes only local interaction

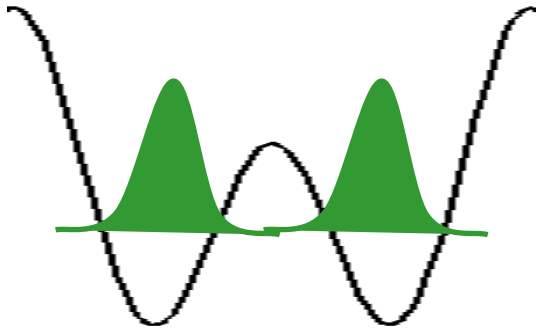

Extended Hubbard model takes into account non-local interaction

$$\hat{H}^{\mathrm{EHM}} = \hat{H}^{\mathrm{HM}} - \Delta J \sum_{\sigma\neq\sigma'} \left(\hat{n}_{\sigma\mathrm{L}} + \hat{n}_{\sigma\mathrm{R}}\right)\left(\hat{a}^{\dagger}_{\sigma'\mathrm{L}}\hat{a}_{\sigma'\mathrm{R}} + \hat{a}^{\dagger}_{\sigma'\mathrm{R}}\hat{a}_{\sigma'\mathrm{L}}\right)$$

$$+ U_{\mathrm{LR}} \sum_{\sigma\neq\sigma'} \Big(\hat{n}_{\sigma\mathrm{L}}\hat{n}_{\sigma'\mathrm{R}} + \hat{a}^{\dagger}_{\sigma\mathrm{L}}\hat{a}^{\dagger}_{\sigma'\mathrm{R}}\hat{a}_{\sigma'\mathrm{L}}\hat{a}_{\sigma\mathrm{R}}$$

$$+\frac{1}{2}\hat{a}^{\dagger}_{\sigma\mathrm{L}}\hat{a}^{\dagger}_{\sigma'\mathrm{L}}\hat{a}_{\sigma'\mathrm{R}}\hat{a}_{\sigma\mathrm{R}} + \frac{1}{2}\hat{a}^{\dagger}_{\sigma\mathrm{R}}\hat{a}^{\dagger}_{\sigma'\mathrm{R}}\hat{a}_{\sigma'\mathrm{L}}\hat{a}_{\sigma\mathrm{L}}\Big)\ ,$$

Beyond the basic Hubbard model

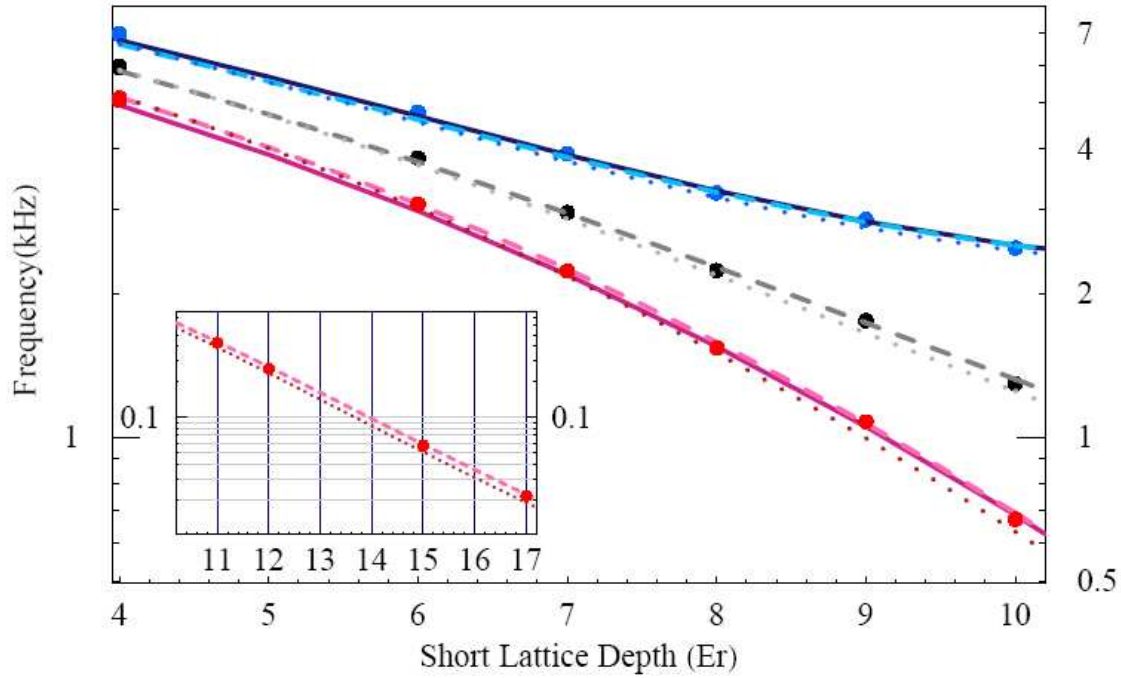

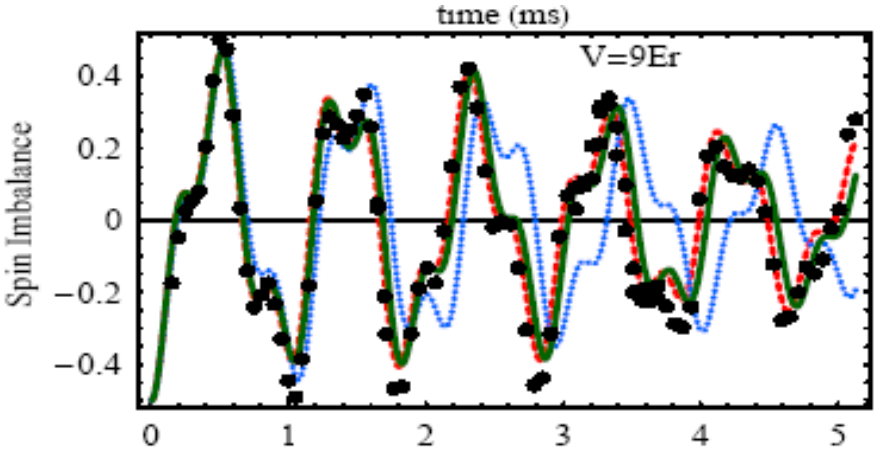

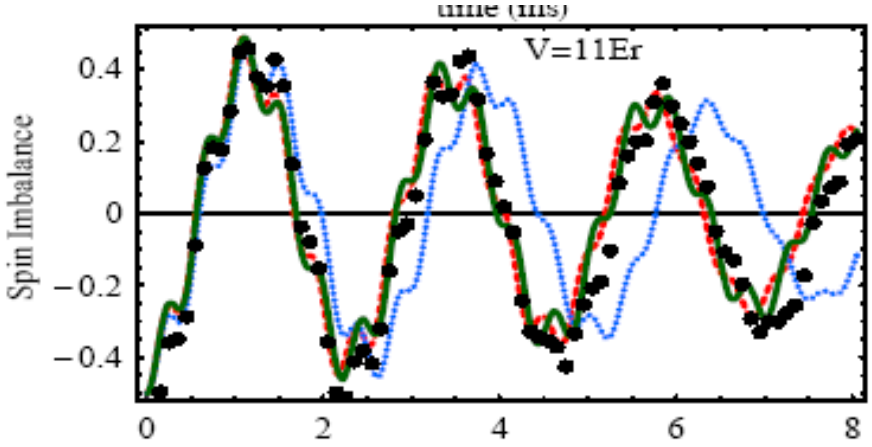

Observation of superexchange in a double well potential. Reversing the sign of exchange interactions

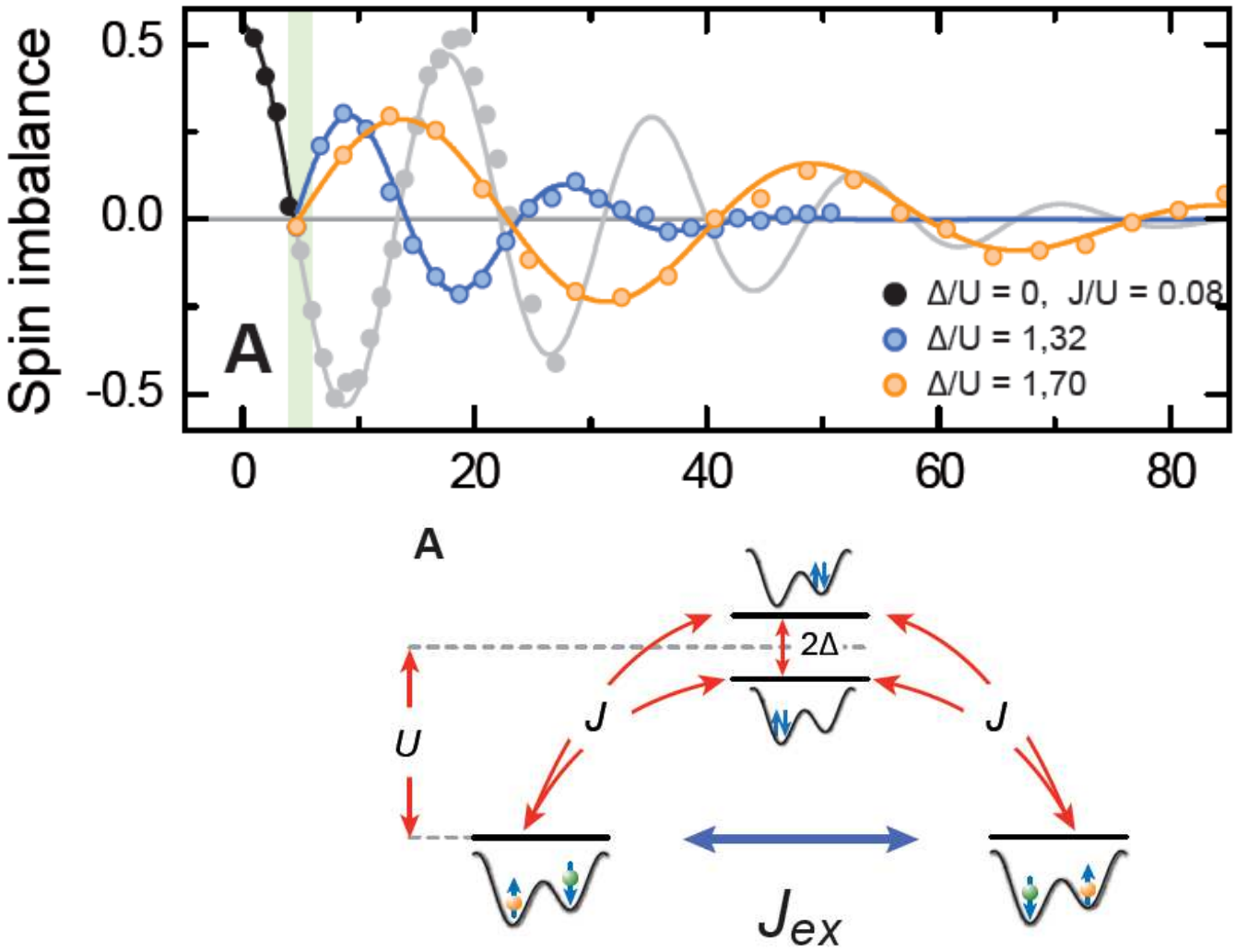

Summary

Dipolar interactions in spinor condensates

Larmor precession and dipolar interactions. Roton instabilities.

Following experiments of D. Stamper-Kurn

Many-body decoherence and Ramsey interferometry

Luttinger liquids and non-equilibrium dynamics.

Collaboration with I. Bloch's group.

Superexchange interaction in double well systems

Towards quantum magnetism of ultracold atoms.

Collaboration with I. Bloch's group.